MICROSTRIP PATCH ANTENNA ARRAY FOR LTE AND MIMO APPLICATIONS

Submitted by:

Muhsin Ali

2011-NUST-MS PHD- Elec (Comm-N)-11

Supervised by:

Dr. Khawaja Bilal Ahmed Mahmood

THESIS

Submitted to:

Department of Electronic and Power Engineering

Pakistan Navy Engineering College, Karachi

National University of Sciences and Technology, Islamabad, Pakistan

In partial fulfillment of requirements for the award of the degree of

MASTER OF SCIENCE IN ELECTRICAL ENGINEERING

Specialization in Communication

March 2013


بسم الله الرحمن الرحيم

ACKNOWLEDGMENTS

All praise and thanks to the Almighty whom we seek help and guidance for sustenance. I would like to show my sincere appreciation to my thesis supervisor Dr. Khawaja Bilal Ahmed Mahmood for his immense guidance, suggestions and wise reproach throughout the course of thesis. He not only guided me but also assisted in practical matters. His timely and efficient involvement helped me conclude my research work and I express my sincere appreciation for his support. I would also like to express my gratefulness to Head of the Department Cdr. Dr. Ataullah Memon for guiding and helping me in getting project funds and showing his interest and permitting me to visit SEECS-NUST to complete my hardware. I also thank Cdr. Dr. Sajjad Hyder Zaidi on this matter. It is also worthy to present my thanks to Head of the RIMMS lab, SEECS-NUST Dr. Muneer Ahmad Tarar for giving prioritized access to the necessary equipment to test my hardware.

Finally, I feel pleasure to thank my GEC committee members, my colleagues and all those who have helped me in any way for making this research a success.

ABSTRACT

The existing and emerging wireless communication standards assume that the clients use omni-directional antennas; radiating in all directions. This has been a barrier to network capacity and client efficiency. MIMO is considered as a key smart antenna technology, to improve the capacity of a communication channel at a greater extent as compared to Single Input Single Output (SISO) and Single Input Multiple Output (SIMO) techniques. MIMO is a technology which uses multiple antennas both at transmitter and receiver to increase the overall data transmission rate and provide higher spectral efficiency. MIMO antennas have been an area of extensive research all over the world during recent years because of its ability to increase the system capacity without increasing the channel bandwidth. The LTE based mobile devices recommend the use of small-scale and multi-band MIMO antennas. The primary aim of this project is to design a dual-band antenna array for LTE and MIMO applications. The antenna will cover two 4G LTE frequency bands of 2.1 GHz (LTE Band-1) and 3.5 GHz (LTE Band-22). These bands are allocated by Pakistan Telecommunication Authority (PTA) for the deployment and development of 3G/4G cellular communication in Pakistan.

TABLE OF CONTENTS

List of Figures

List of Tables

Chapter 1

Introduction

Multiple Input Multiple Output (MIMO) is considered as a key smart antenna technology, to improve the capacity of a communication channel at a greater extent as compared to Single Input Single Output (SISO) and Single Input Multiple Output (SIMO) techniques [1, 2]. MIMO technology makes it possible to transmit multiple data streams over a same frequency channel without increasing the physical bandwidth of that channel [3]. It utilizes multiple antenna elements both at transmitter and receiver ends to increase the data transmission rate by providing higher spectral efficiency [1]. The 4G cellular mobile communication standard, Long Term Evolution (LTE) [4], utilizes MIMO to provide improved data rates. With the help of MIMO technology 4G LTE can provide downlink data rates of up to 1Gbps. The LTE based mobile devices and other 4G-handled equipment recommend the use of small-scale and multi-band MIMO antennas.

In this thesis, U-slot rectangular microstrip patch antenna arrays are designed, simulated, fabricated and characterized. The antenna covers two 4G LTE frequency bands of 2.1 GHz (LTE Band-1) and 3.5 GHz (LTE Band-22). These bands are allocated by Pakistan Telecommunication Authority (PTA) for the deployment and development of 4G LTE technology in this region. The bandwidth requirements for these two frequency bands are 60 MHz and 80 MHz, respectively. The simulations of the proposed antenna are performed in Agilent Advanced Design System (ADS) [5], an electromagnetic simulator. Its simulation tool is based upon full-wave Method of Moment (MoM) numerical technique.

1.1 Multiple Input Multiple Output

Multiple Input Multiple Output, or MIMO, is a form of smart antenna technology in which multiple antennas are used at both the transmitter and receiver ends to improve the data rate of a communication system. One of the main advantages of MIMO is that it increases data throughput and link range at a significant level without any increase in the channel bandwidth or transmit power [3]. The same total transmit power is spread over each of the antennas, which improves the spectral efficiency. Hence, providing more number of bits/sec/Hz of the bandwidth [3]. The gain of each of the antenna element in the array is combined to form an array gain, which is much higher than a single element antenna. Because of all these interesting properties, MIMO technology has been an integral part of modern high speed communication standards like 4G WiMAX and LTE, IEEE 802.11n and HSPA+ [4].

The generic form of MIMO antenna system is shown in Fig. 1.1 (a). The transmitter is shown by *Tx* and the receiver is shown by *Rx*. It can be seen that multiple antennas are used at both the ends. Theoretically, the link throughput efficiency of a MIMO system is directly proportional with the number of antennas, *n*. The main concept behind the operation of MIMO is spatial multiplexing (SM). The SM is a transmission technique in which encoded data signals (also known as streams) can be transmitted separately and independently via each of the multiple transmit antennas. The space dimension is multiplexed more than one time. For example, if there are N_t antennas equipped on the transmitter and N_r on the receiver, the maximum number of streams (spatial multiplexing order) that can be generated is:

$$Ns = min\ (N_t, N_r) \tag{1.1}$$

It means that, ideally, a total of *Ns* independent parallel data streams can be transmitted simultaneously. This implies an *Ns* increase in spatial efficiency. The detailed MIMO transmission is depicted in Fig. 1.1 (b). The N_t antennas at transmitter, *Tx*, are sending data streams. There are N_tN_r transmission paths between N_t transmit antennas and N_r receiving antennas. Each of the receive antennas, N_r, receives a copy of N_t transmitted streams. The receiver gets the signal in the form of a vectors and and converts them into original information.

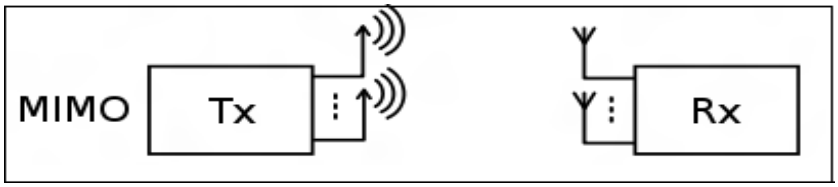

(a)

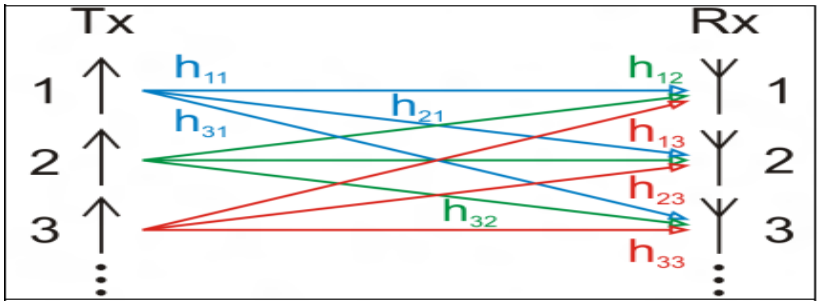

(b)

Figure 1.1: (a) General form of MIMO antenna system (b) Detailed depiction of MIMO transmission [3]

1.2 Long Term Evolution

Long Term Evolution [4, 6], or LTE, is a global standard for high speed wireless communication for mobile phone. It falls under fourth generation of mobile broadband, often referred as 4G LTE. Launched in 2009, it is the fastest developing mobile communication standard. The standards of the LTE are defined by 3rd Generation Partnership Project (3GPP).

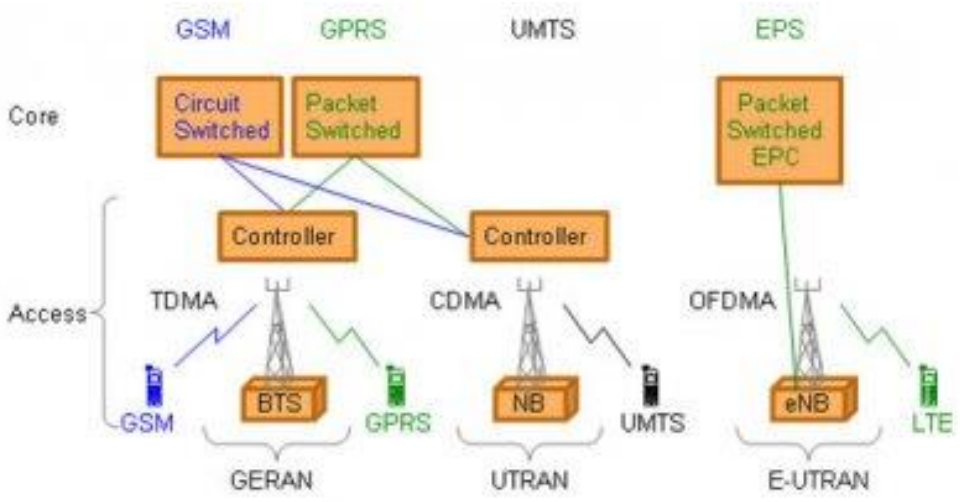

Figure 1.2: Mobile networks from GSM to LTE [9]

Although introduced as a 4G network, the first marketed version of the LTE did not meet the data rate requirements specified by 3GPP consortium, it was being described as 3.9G (beyond 3G but pre 4G). Therefore, an improved version of LTE was introduced in 2011 which is known as LTE-Advanced [7, 8]. The architecture of the LTE is based on and an evolution of 2G and 3G standards like Global Systems for Mobile communications (GSM) and Universal Mobile Telecommunication System (UMTS), as shown in Fig. 1.2. Along with some major core network improvements, it also uses a different radio interface to increase the system capacity. One goal of LTE was to redefine the network architecture of mobile communication systems to an all-IP based system with very low latency as compared to 3G architecture. This IP-based architecture is part of the Evolved Packet System (EPS) [9]. Secondly, to exploit the new DSP (digital signal processing) techniques to increase the capacity of data networks. LTE provides peak download data rate of up to 300Mbps and upload data rate up to 75Mbps [4, 9]. Whereas, LTE-Advanced provides an incredible peak data rate for LTE-Advanced of up to 3.3Gbps [4, 8].

The major factor that makes it possible to provide extremely high data rates is the utilization of MIMO techniques. The LTE configuration supports 4 x 4 MIMO antenna configuration utilizing 20MHz of frequency bandwidth and LTE-Advanced supports up to 8 x 8 MIMO with increasing the system bandwidth to 100MHz [4, 7]. A completely new air interface

was defined for LTE known as Evolved Universal Terrestrial Radio Access (E-UTRA). LTE air interface is divide into 43 different frequency bands (Appendix-A).

1.3 Thesis Approach

Until now LTE has not deployed in Pakistan and this is one of the initial efforts to design antennas for LTE frequencies assigned to Pakistan or Asia region. The available LTE based devices cannot operate here because they are designed to operate on other frequency bands. There is a need to develop cost effective antennas according to our needs.

The goal of this thesis is to develop a cost effective dual-band microstrip patch antenna system that can support LTE based transceivers designed for Pakistan. It will be an indigenously designed MIMO antenna system. Because of its dual-band operation, it can be used for multiple applications. The proposed antenna will provide a solution for the antennas for 4G mobile communication systems.

Initially, the different types of patch antenna arrays were simulated using Agilent's ADS software over different substrates. The purpose behind that study was to select an antenna design that should be an optimum solution for our approach. There several types of planar antennas available but we selected the U-slot microstrip patch antenna because of its simple design, availability of design equations and it easily gives multi-band behavior. It is selected as an optimum antenna to meet our goal of designing cost-effective, low-profile and multi-application antenna. After the antenna design, simulations and optimization are completed the antennas will be fabricated and characterized. To achieve high accuracy, the antennas are fabricated by a commercial fabricator and the testing facility available at RIMS, SEECS-NUST is used for measurements and antenna characterization.

1.4 Thesis Organization

This thesis is organized as follows. Chapter 2 consists of an introduction to antenna theory and various types of antennas. Chapter 3 presents a detailed introduction, operation and design procedure of microstrip patch antennas. The theory of microstrip U-slot patch antenna, design and optimization procedures is discussed in chapter 4. Chapter 5 presents the simulation results of single U-slot patch antenna element and then array. Finally, design and simulation results are concluded.

Chapter 2

Antenna Fundamentals

In this chapter, the fundamental concepts and basic terminology of an antenna are presented. Also, some common and most important performance parameters for an antenna are discussed. Finally, some antenna types are discussed.

2.1 Introduction

An antenna is an electrical device that converts electrical energy into electromagnetic waves, and vice versa. It is made to radiate and receive electromagnetic signals. An antenna is essential part of a wireless communication system. While deployed at transmission system, an antenna receives electric energy from the transmitter and radiates in into the space [12, 13]. At receiver, it intercepts the electromagnetic waves, produces voltage at its terminals [13]. The standard definition of the antenna according to IEEE is given by Stutzman and Theile [12] as: “The part of a transmitting or a receiving system that is designed to radiate or receive electromagnetic waves”.

2.2 How Antenna Works

The basic structure of an antenna contains an arrangement of metallic conductors, known as elements, in a specific fashion to a transmitter or a receiver. A pair of conducting wires radiate because of time-varying or accelerating (or decelerating) current. When oscillating current of electrons generated by transmitter is passed through an antenna, it creates an oscillating magnetic field around the antenna elements and electronic charge creates an electric field along it elements. After creating in a proper portion, these fields radiate into the space away from antenna as moving transverse electromagnetic (TEM) waves. No radiation takes place if charges do not move in wire, hence no flow of the current. Also, when the charges are moving with uniform velocity along a straight line, radiation does not occur. But radiation occurs when charges are moving with uniform velocity on a curved patch. According to Balanis, radiation takes place along a straight line if the charges are oscillating with respect to time [13]. During reception, the oscillating electromagnetic field in an incoming wave asserts force on the electrons in the metallic element of antenna, causing them to move back and forth at the frequency of incoming wave, thus creating electric current in antenna.

Fig. 2.1 can help understand antenna radiation in more detail. It shows a two-conductor transmission line, with its ends having an opening in air, connected with a voltage source. The

applied voltage creates electrical field in the transmission line, known as electric lines of force, as shown in Fig. 2.1. This field is sinusoidal in nature. These lines of force displace the electrons in the conductor and this movement of electrons produces a current which in turn creates a magnetic field. These electric and magnetic fields, when combined, generate an electromagnetic field inside the transmission line and travel through it. After reaching the antenna (the open portion of the transmission lines) they are radiated into the free space forming close loops [12-14].

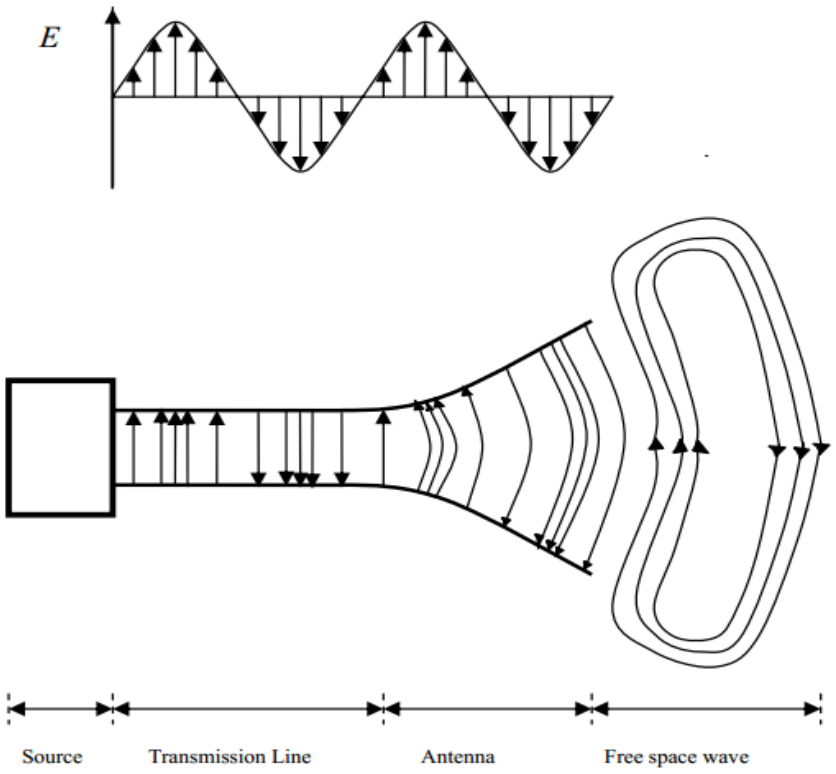

Figure 2.1: Antenna Radiation [11]

2.3 Near and Far Field Regions

The near field and far field are the regions of varying electromagnetic field around an antenna. The field regions define how the properties of an electromagnetic field change with respect to distance from the source. The field patterns are related with two different types of energies; radiating energy and reacting energy. The surrounding space is divided into three regions as shown in Fig. 2.2.

- Reactive near-field region: This region is dominated by the reactive field. The field in this region appears as reactance because it oscillates towards and away from antenna. Energy is stored in this region and does not dissipate. The distance of outermost boundary for this region is given by $R1 = 0.62\sqrt{D^3/\lambda}$, where R1 is distance of field boundary from the surface of antenna, *D* is the maximum dimension of antenna and λ is the wavelength of electromagnetic field.

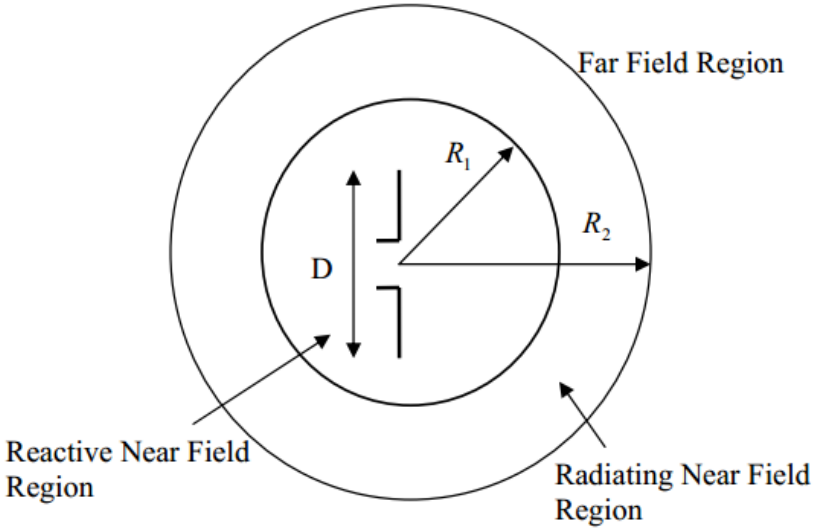

Figure 2.2: Antenna Field Regions [11]

- Radiating near-field region: The radiating near-field region is also known as Fresnel region. It lies between the reactive near-field region and far field region. The reactive fields are smaller in region than in reactive near-field region. This region is dominated by the radiating fields. The distribution of the angular field in this region is a function of distance from the antenna. The range of the outermost boundary for this region is given by $R2 = 2D^3/\lambda$, where R2 is the distance of field boundary from surface of the antenna.

- Far field: The far field region is also known as Fraunhofer region [16]. There are no reactive fields in this region. In the region far away from charge separations and currents, the electromagnetic field is affected by the charge in other fields and it is no longer affected by charge and current at source. The distant part of electromagnetic field becomes radiating field (also called far-field). Contrary to previous field types, the angular field distribution is independent of the distance from antenna in far-field region. The region beyond $R2 = 2D^3/\lambda$ is considered as far-field region.

2.4 Reciprocity

Usually, the electrical characteristics of an antenna are identical whether it is transmitting or receiving. The receiving pattern of an antenna when used for reception is exactly same as its radiation pattern when used for transmission. The conductor of which the antenna is made should have same response to an electric field or current in one direction as it has to an electric field or current in another direction. Because of this property no distinction is made between transmitting and reception properties of an antenna. Same antenna can be used for transmission as well as reception.

2.5 Antenna Performance Parameters

Antennas are characterized on the basis of number of different performance parameters. These parameters are essential in designing and selecting antennas for specific applications. Some antenna parameters are discussed briefly.

2.5.1 Radiation Pattern

The radiation pattern of an antenna is a function of far-field radiation properties or graphical representation of radiation properties as a function of spatial coordinates. It is generally represented by three dimensional graph or polar plots [13-15]. The radiation properties which are considered for radiation pattern include radiation intensity, flux density, field strength, phase, polarization and directivity. An isotropic antenna is a theoretical concept which radiates equally in all directions. The radiation pattern of isotropic antenna would look like a sphere. If power *P* is emitted by an isotropic antenna in a region of radius *r*, the power density is given as [12]:

$$S = \frac{P}{area} = \frac{P}{4\pi r^2} \tag{2.1}$$

The radiation intensity for isotropic antenna U_i is given as [12]:

$$U_i = \frac{P}{r^2 S} = \frac{P}{4\pi} \tag{2.2}$$

It is impossible to design an isotropic antenna but there are some approximations of it known as omnidirectional antennas. The radiation pattern of an omnidirectional antenna, when plotted, looks like a donut. The general form of radiation pattern of many antennas is shown in Fig. 2.3. The portion where most of the radiated power lies is known as “maxima” “main lobe. Nulls are the portions where no power lies. Side lobes are smaller lobes which are separated by nulls. The back lobe or opposite lobe lies on the opposite side of the main lobe. Another

important terminology for radiation pattern is half power beam width (HPBW) which is defined as the angle subtended by half power points on main lobe.

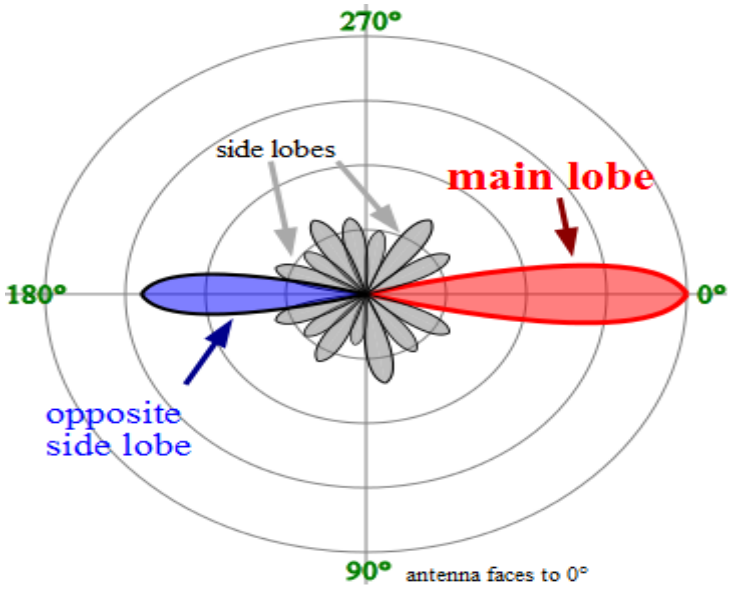

Figure 2.3: General form of antenna radiation pattern [11]

2.5.2 Directivity

According to [13] the antenna directivity is defined as "the ratio of the radiation intensity in a given direction from the antenna to the radiation intensity averaged over all directions". In simple words, directivity of an antenna is the ratio of radiation intensity of an antenna to radiation intensity of an isotropic antenna in a direction. Mathematical expression of directivity is given as

$$D = \frac{U}{U_i} = \frac{4\pi U}{P} \tag{2.3}$$

where D is antenna directivity

U_o is radiation intensity of antenna

U_i is radiation intensity of isotropic antenna

P is power radiated by antenna

In cases where the direction of the directivity is not indicated, the direction of maximum radiation intensity is implied. The maximum directivity is expressed as

$$D_{max} = \frac{U_{max}}{U_i} = \frac{4\pi U_{max}}{P} \tag{2.4}$$

Where D_{max} is maximum directivity

U_{max} is maximum radiation intensity

Since the directivity is a ratio, it is a dimensionless quantity. It is expressed in dBi. The "i" refers to isotropic antenna. Narrower the front lobe of an antenna, greater is the directivity and vice versa. For a given polarization, the partial directivity is the part of radiation intensity in that polarization, divided by total radiation intensity averaged over all directions.

2.5.3 Gain

The gain of an antenna is closely related to its directivity. It measures the degree of directivity of an antenna's radiation pattern. Gain is defined gain as "the ratio of the radiation intensity in a given direction, to the radiation intensity that would result if the power fed to the antenna were radiated isotropically" [14]. A high gain antenna will radiate more in a specific direction. A high gain antenna will provide increased range and better signal quality than isotropic antenna in a particular direction.

When referenced with an isotropical antenna, the antenna gain is given in dBi. Mathematically, gain is expressed as

$$D = 4\pi \frac{radiation\ intensity}{total\ input\ power} = 4\pi \frac{U(\Theta,\ \phi)}{P_i} \tag{2.5}$$

2.5.4 Return Loss (RL)

Return loss characterizes the relation between the input and output in a transmission line, especially when the load is mismatched and not all power is delivered to the load (antenna). For mismatched loads, some fraction of delivered power is reflected back to the source. The return loss shows the amount of power transferred to the load. The return loss is given by:

$$RL = -20\log|\Gamma| \quad \text{(dB)} \tag{2.6}$$

where

$$|\Gamma| = \frac{V_0}{V_{in}} = \frac{Z_L - Z_0}{Z_L + Z_0} \tag{2.7}$$

$|\Gamma|$ = magnitude of reflection coefficient
V_o = reflected voltage
V_{in} = input voltage
Z_L and Z_o are the load and characteristic impedances.

For the case of perfect matching when no power is reflected back, Γ=0 and RL= ∞. Whereas, Γ=1 and RL= 0 imply that all of the transmitted power is reflected back to the source. For practical applications, an RL of -10 dB or below is considered as acceptable.

2.5.5 Input Impedance

The antenna input impedance is defined as "the impedance presented by an antenna at its terminals or the ratio of voltage to current at pairs of terminals" [13]. It can also be considered as the ratio of electric field to magnetic field at a point. Mathematically, input impedance is written as:

$$Z_{in} = R_{in} + jX_{in} \quad (2.8)$$

where Z_{in} is the antenna impedance

R_{in} is the antenna resistance

X_{in} is the antenna reactance

R_{in} is composed of two parts, radiation resistance R_r and loss resistance R_L. The power that is acutally radiated by antenna is related with R_r and the power which is dissipated as heat or other losses is related with R_L. The imaginary part, X_{in}, is related to the power stored in near field of the antenna.

2.5.6 Antenna Efficiency

The parameter of antenna efficiency considers the amount of losses at antenna terminals and physical structure of antenna. These losses may include:

- Reflections due to mismatch between the transmitter and receiver
- I^2R (power losses)

So, overall efficiency is given by:

$$e_t = e_r\, e_c\, e_d \quad (2.9)$$

where e_t = total efficiency

e_r = reflection efficiency = $(1 - |\Gamma^2|)$

e_c = conduction efficiency

e_{ss} = dielectric efficiency

2.5.7 Polarization

Polarization is a parameter which tells about the orientation of the electric field of an electromagnetic wave in far-field region. In [13] it is defined as "the property of an electromagnetic wave describing the time varying direction and relative magnitude of the electric field vector". The position and direction of electric field wave is taken with reference to the earth's surface to determine its polarization. When direction of antenna radiation is not stated, the polarization is taken in the direction of maximum gain. Some common types of polarization include linear, circular, elliptical, circular left hand, circular right hand, elliptical left hand and elliptical right hand polarization.

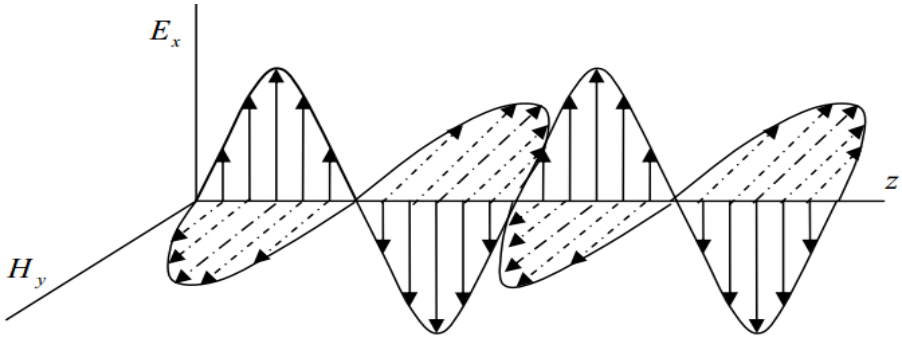

Figure 2.4: Linearly polarized electromagnetic wave [13]

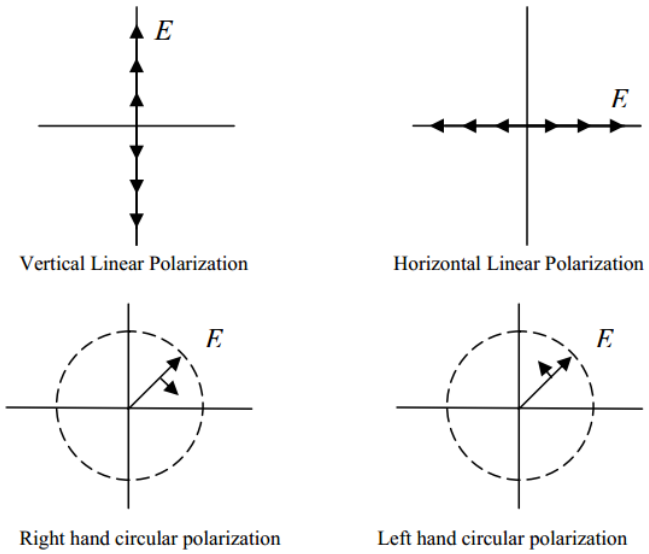

Figure 2.5: Linear and circular polarizations [11]

Fig. 2.4 shows a linearly polarized wave. In linear polarization, the path of electric field vector is back and forth along a straight line. Whereas in circular polarization, the magnitude of the electric field vector remains constant but it rotates around a circular path. When the vector routes counterclockwise it is called left hand circular polarization and when it rotates clockwise it is called right hand circular polarization, as shown in Fig. 2.5.

2.5.8 Voltage Standing Wave Ration (VSWR)

Maximum power transfer from transmitter to the antenna should take place in order for antenna to operate efficiently. This can only take place if the input impedance of antenna, Z_{in}, matches with impedance of source or transmitter, Z_S. The power transfer theorem states that "only if impedance of the transmitter is a complex conjugate of the impedance of the antenna, the maximum power can be transferred, or vice versa. This condition is written mathematically as:

$$Z_{in} = Z_S \tag{2.10}$$

where $Z_{in} = R_{in} + jX_{in}$

$Z_S = R_S + jX_S$

When this condition is not met, some of the power reflects back to the source and which, in turn, create standing waves in transmission line. These standing wves are characterixxed by a term known as voltage standing wave ratio (VSWR). VSWR is given by [15] as:

$$VSWR = \frac{1+|\Gamma|}{1-|\Gamma|} \tag{2.11}$$

where Γ is called reflection coefficient

Basically, VSWR is the measure of ismatch between transmitter and antenna. Lesser the value of VSWR, lower is the mismatch and vice versa. For a perfect match, the VSWR is unity.

2.5.9 Bandwidth

Antenna bandwidth is defined by [13] as "the range of frequencies for which the performance of antenna conforms to a specific". The bandwidth of an antenna can be thought as the range of frequencies on both sides of the counter frequency where the antenna parameters are close to those obtained at center frequency. These antenna parameters include

input impedance, radiation pattern, Beamwidth, polarization or gain. Bandwidth of broadband and narrowband antenna is obtained by equations 2.12 and 2.13, respectively.

$$BW_{broadband} = \frac{f_H}{f_L} \tag{2.12}$$

$$BW_{narrowand}(\%) = \left[\frac{f_H - f_L}{f_C}\right]100 \tag{2.13}$$

Where f_H = upper frequency

f_L = lower frequency

f_C = center frequency

For a broadband antenna, $\frac{f_H}{f_L} = 2$. Antenna performance in required frequency band is measured by its VSWR in that band. A *VSWR ≤ 2* (*RL ≤ -10 dB*) ensures satisfactory performance. Fig. 2.6 shows how to measure antenna bandwidth from its return loss plot.

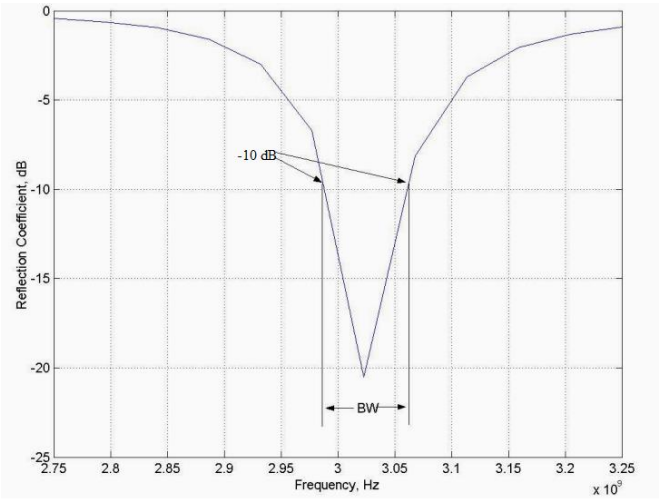

Figure 2.6: Measuring antenna bandwidth from return loss plot [11]

2.5.10 Beam Efficiency

Beam efficiency is a parameter used to judge the quality of transmitting and receiving antennas. It is given as:

$$B = \frac{Power\ transmitten\ (received)\ within\ cone\ angle\ \theta}{Power\ transmitten\ (received)\ by\ the\ antenna} \tag{2.14}$$

Where θ is the half angle of the antenna radiation cone

2.6 Types of Antenna

Several types of antenna are available with different sizes and shapes to suit for the variety of applications. The size, shape and the material which it is made of can determine its basic characters. Some common types of antenna are discussed below.

2.6.1 Half Wave Dipole Antenna

A half wave dipole antenna is made of two metal conductors of wire or rod arranged in line with each other, with a small space between them. One of the two elements is center-fed driven element. Each of these elements is of the length of quarter wavelength which makes total antenna length of half wavelength or λ/2, as shown in Fig. 2.7. Dipoles can be shorter or longer than λ/2 according to required antenna performance but half wavelength is widely used.

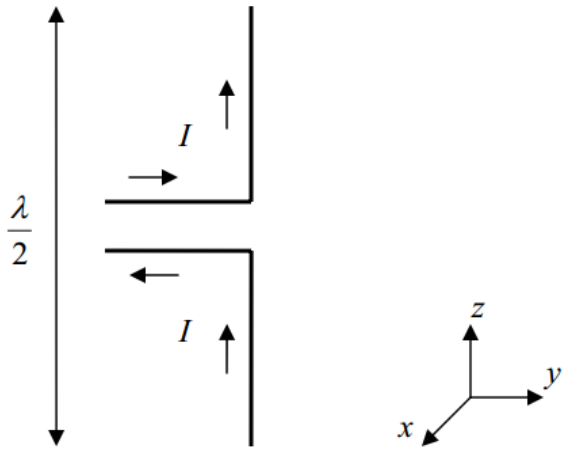

Figure 2.7: Half wave dipole antenna [12]

As shown in Fig. 2.7, the dipole is fed by a two-wire transmission line. We can see that current in both the wires is opposite in direction but of sinusoidal distribution and equal amplitude. No radiation occurs in transmission line due to cancelling effect. Whereas the current in the dipole flows in same direction and produce radiation. The vertical orientation of dipole produces horizontal radiation and horizontal orientation produces vertical radiation. A dipole antenna has a gain of about 2.15 dBi, bandwidth of 10% and radiation resistance of 73 Ω [10]. Radiation pattern of a half wave dipole antenna is shown in Fi. 2.8.

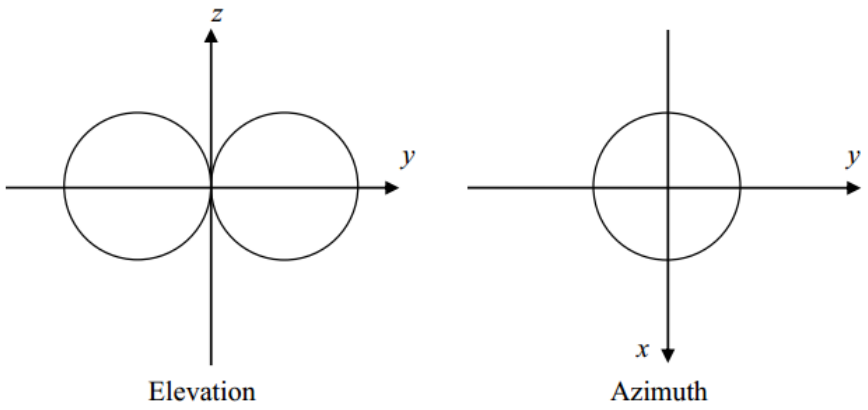

Figure 2.8: Radiation pattern of a half wave dipole antenna [12]

2.6.2 Monopole Antenna

A monopole antenna consists of a straight rod-shaped conductor mounted perpendicularly over a conducting known as a ground plane. Fig. 2.9 shows a typical monopole antenna. The monopole antenna is formed by applying image theory to a dipole antenna which states that if a conducting place is placed below a rod-shaped metallic element carrying a current, an image of the conducting element is formed below the plane. The combination of element and its image is identical to a dipole of length *λ/2* . The length of element is *λ/4*. In this case, the radiation only occurs above the ground plane [12].

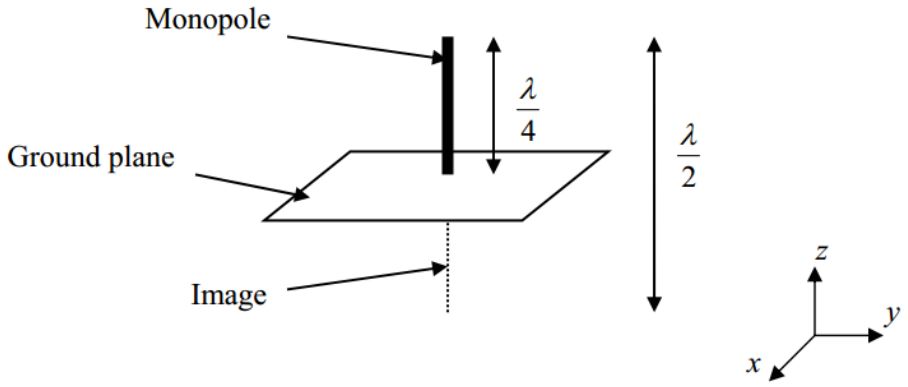

Figure 2.9: Monopole antenna [12]

The quarter wave monopole antenna is an approximation of half wave dipole. As compared to a dipole, the directivity of a monopole antenna is doubled and radiation resistance is halved. The monopole antenna is very useful in mobile applications because it is half the size

of dipole antenna. While used on car, the body of car acts as ground plane. The gain of quarter wave monopole id 5.19 dBi and its radiation resistance is 36.8Ω [12, 13]. Electrically small ground plane is sometimes used to tilt the direction of maximum radiation. The radiation pattern of a monopole antenna is shown in Fig. 2.10.

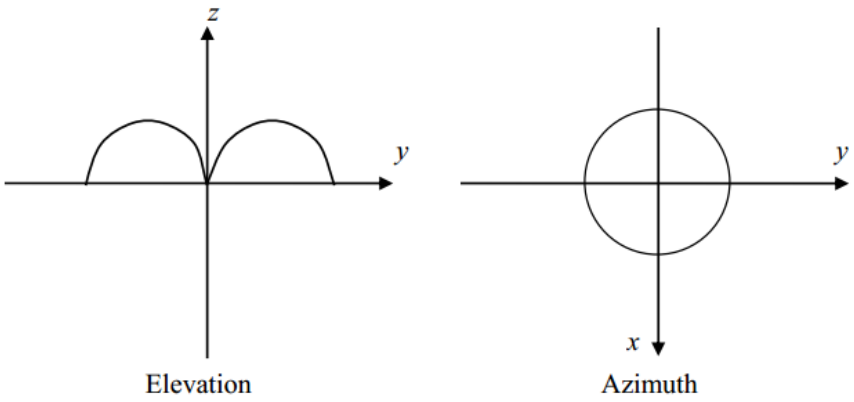

Figure 2.10: Radiation pattern of monopole antenna [12]

2.6.3 Loop Antennas

A loop antenna consists of a wire, tube or other metal bent into a closed circular or a rectangular shape with its ends (terminals) connected to a transmission line [14]. Loop antennas are of two types: small loop antennas and large loop antennas, shown in Fig. 2.11. The loop circumference of a small loop antenna is much smaller as compared to wavelength ($L << \lambda$) [12, 16]. To ensure a constant current distribution across the loop, it should be of the length of $\lambda/10$ or less [5]. When the circumference of a loop antenna is approximately equal to the wavelength, it is said to be a large loop antenna.

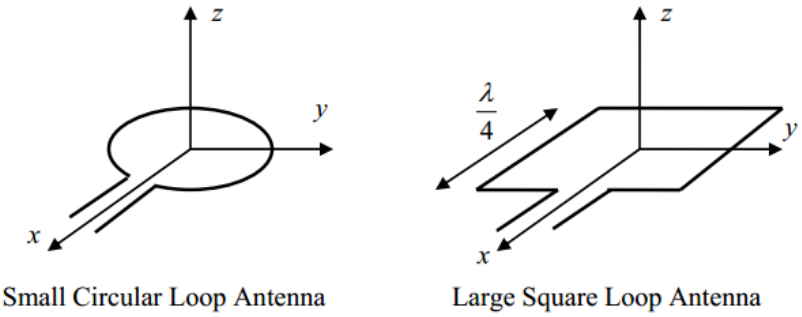

Figure 2.11: Loop antennas [11]

Small loop antennas usually have poor efficiency and are mainly used for receivers at low frequencies. When the loop size is increased, the standing waves start to develop in current and antenna start to behave like large loop or self-resonant antenna. Filling loop core with ferrite helps increasing performance of a loop antenna because it increases the radiation resistance.

The loop antennas have a usual gain of 3dBi and bandwidth of 10% [12]. The large or self-resonant loop antenna of the length of one wavelength, compared to dipole, transmits less toward ground or sky. This property gives it a higher gain in horizontal direction. Large loop antenna radiates in direction normal to the plane of loop. Polarized of such antenna is not known from its orientation, rather it depends upon feed point. When it is fed from inside, the polarization becomes vertical and if fed at bottom it will be horizontally polarized. Better directivity can be achieved by increasing loop circumference up to 3 or 5 wavelengths. It can be noticed from Fig. 2.12 that radiation patter of large loop antenna is different than that of small loop antenna.

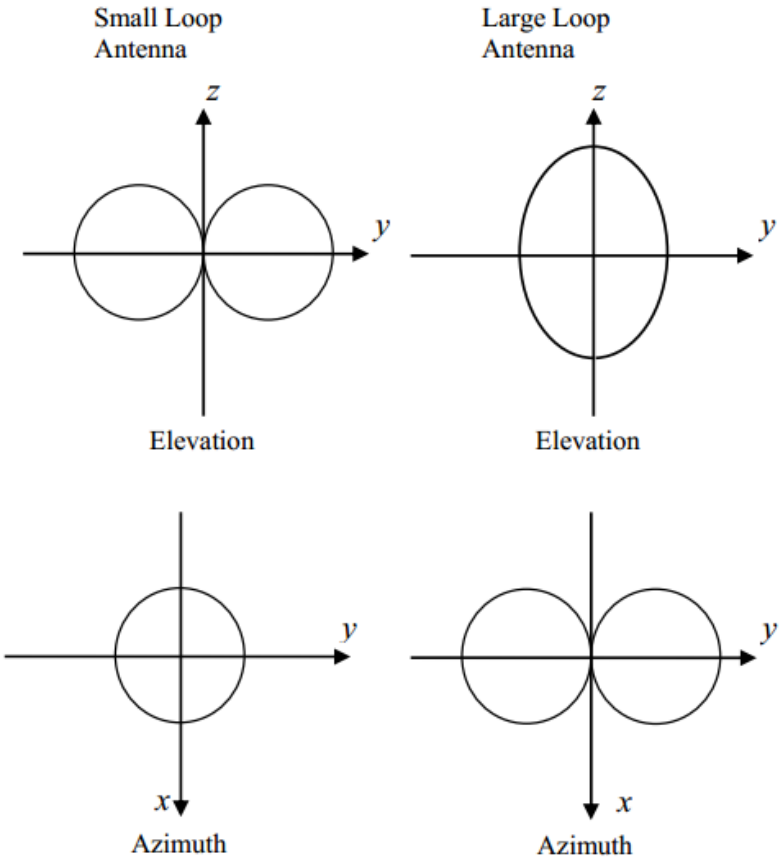

Figure 2.12: Radiation patters of small loop and large loop antenna [11]

2.6.4 Helical Antenna

A helical antenna, also known as helix, is an antenna consisting of a conducting wire wound in the shape of a helix, mounted over a ground plane. The feed line is connected between ground and bottom of the helix. Fig. 2.13 shows a common helix antenna. The two principal modes of helical antennas are normal mode (broadside radiation) and axial mode (endfire radiation).

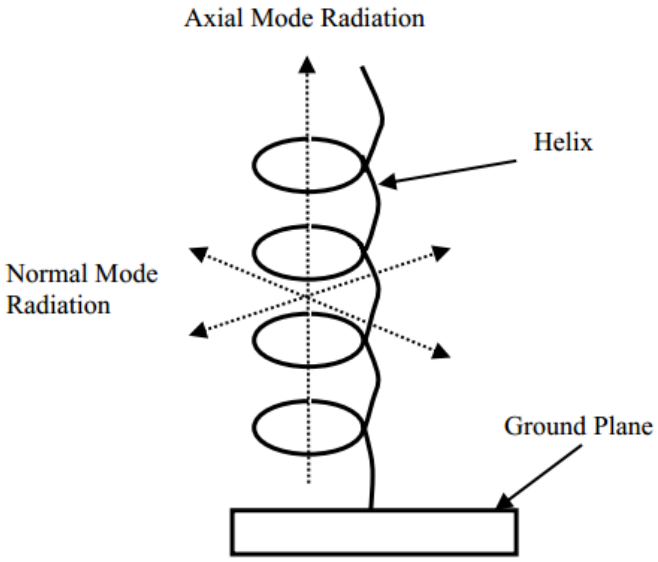

Figure 2.13: Helical antenna [12]

The helical antenna operates in normal mode when its dimensions are small as compared with the wavelength. In this mode the antenna acts as electrically short dipole or monopole and its radiation pattern is omnidirectional with maximum radiation in direction of right angles to the helix axis and minimum in the direction of helix. The normal mode usually provides low bandwidth.

The helix operates in axial mode if its size is comparable to or above the wavelength. The antenna radiates a main directional beam along the axis of the helix. The waves in this mode are circularly polarized. The circular polarization is useful where the relative polarization of transmitting and receiving antenna is hard to maintain. The ground plane acts as a reflector which reflects the waves forward to make it directional such as in space communication. It provides gain of up to 15dBi and bandwidth ratio of 1.78:1 as compared to normal mode helix [12]. The antenna can be made more directional by increasing the number of turns. The radiation patter of both the modes is shown in Fig. 2.14.

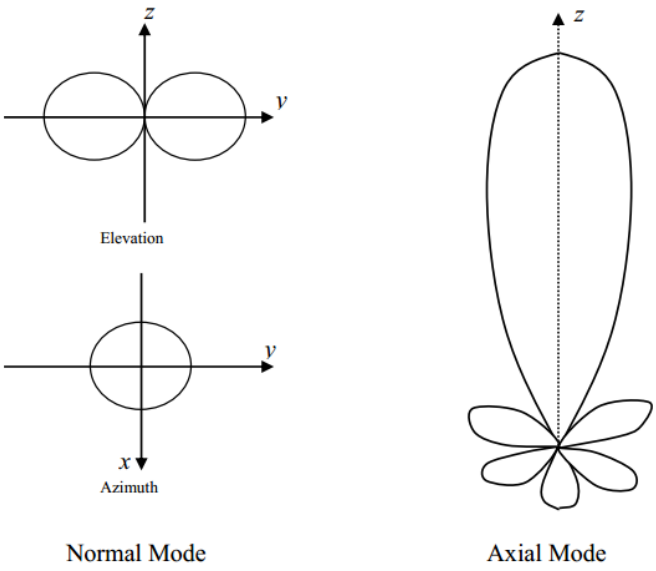

Figure 2.14: Radiation pattern of normal and axial mode helical antenna [12]

2.6.5 Horn Antennas

A horn antenna is made of a metallic waveguide shape like horn to focus radio waves in a beam. The walls of a horn are flared outwards which form a structure like megaphone [12, 13], as shown in Fig. 2.15. Horns antennas are usually used for UHF and microwave frequencies (above 300 MHz). Because the waveguides are difficult to control and their size is inversely proportional to the frequency that means their size at lower frequency is very large. At these frequencies, they are also used as feeders for large antennas such as parabolic antennas and radio telescope. The horn antennas are also considered as standard calibration antennas to measure gain of other antennas.

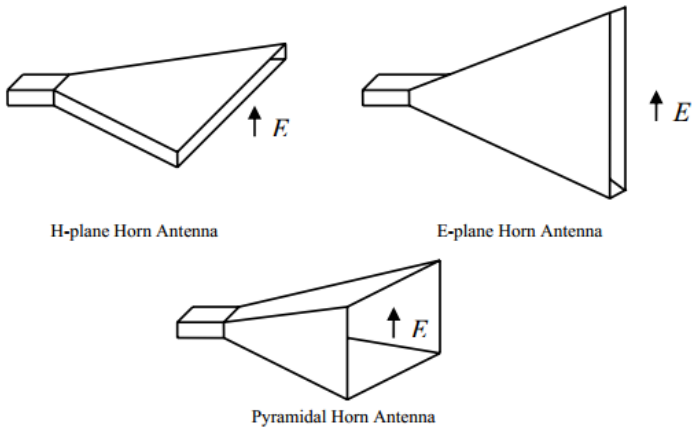

Figure: 2.15 Horn antennas [12]

Three basic types of horn antenna are shown in figure above which are fed by rectangular waveguides. Apart from these, the aperture of horn antennas can be circular and elliptical. The horn antennas can radiate over a wide range of frequencies since they have no resonant elements. In excitation with dominant waveguide mode, E-plane is vertical and H-plane is horizontal. A horn with one pair of sides flared and other being parallel is known as sectorial horn. A sectorial horn with flared E-plane is called an E-plane horn. If the flaring occurs in the direction of H-plane, it is called an H-plane horn. The usable bandwidth of a horn can reach up to order of 20:1 (for example from 1 GHz to 20 GHz). The typical gain of a horn is 10 – 20dBi and can reach up to 25dBi in some cases [12]. They also provide low VSWR over the usable bandwidth. The input impedance may vary slowly over wide frequency ranges.

In above sections, some commonly used antennas were discussed. Another important and widely used antenna, which is selected for this thesis work, is microstrip patch antenna. A detailed discussion of microstrip patch antenna, its types and advantages are presented in next chapter.

Table 1: Summary of common antenna types

Antenna Type	Typical Gain (dBi)	Typical Impedance Bandwidth (%)	Common Applications	Reference
Half-wave Dipole Antenna	2.15	10	Wi-Fi, MiMAX, TV	[12]
Monopole Antenna	2 - 6	10	FM/AM broadcasting, cell phone, Wi-Fi	[13]
Loop Antenna	3	10	Radio direction finding (RDF), aircraft, UHF transmitter	[12]
Helical Antenna	15	53	Satellite communication, AM broadcast, RFID	[14]
Horn Antenna	5 - 20	67	Radar, Satellite dishes, radio telescope,	[11]

Chapter 3

Microstrip Patch Antenna

In this chapter, an introduction to microstrip patch antenna is given along with its advantages and disadvantages. After that, some feeding methods are also discussed. Finally, detailed explanations about the theory and design procedure of a microstrip patch antenna are given.

3.1 Introduction

A microstrip patch is a type of a planar antenna which consists of a radiating patch mounted on the surface of a material. The material is a dielectric substance whose one side is metal-plated which serves as ground plane for antenna [17]. The patch element is a thin layer of a conductor, copper in most cases. The patch is mounted over dielectric substance by photo-etching method [17]. A typical rectangular microstrip patch antenna is shown in Fig. 3.1. It can be seen that a patch of length *L*, width *W* and thickness *t* is placed over a substrate of height *h* and dielectric constant ε_r.

The antenna radiates when the length of the patch is nearly equal to half of the wavelength, *λ/2* [17, 18]. The fringing field is created between patch edges and ground plane which causes radiation. The radiation at antenna edges makes patch antenna electrically larger than its physical dimensions.

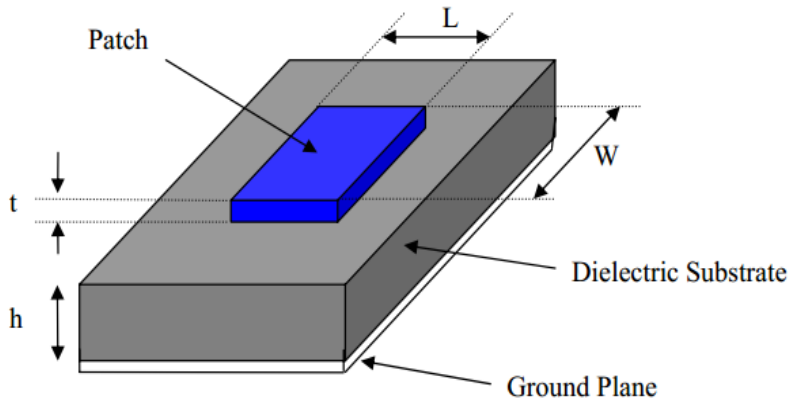

Figure 5.1: Rectangular microstrip patch antenna [11]

Because of this reason, the length of microstrip patch slightly shorter than one-half wavelength is used in order for antenna to radiate. For better antenna performance, better radiation and higher bandwidth, a substrate with low dielectric constant and higher thickness is required [13]. But this kind of antenna structure leads to larger size of the patch. The patch can be made smaller with higher dielectric constant values but this will reduce antenna bandwidth. Therefore, a trade-off is required between antenna size and its performance. Various shapes of microstrip patch element are available each with different properties and performance, as show in Fig. 3.2.

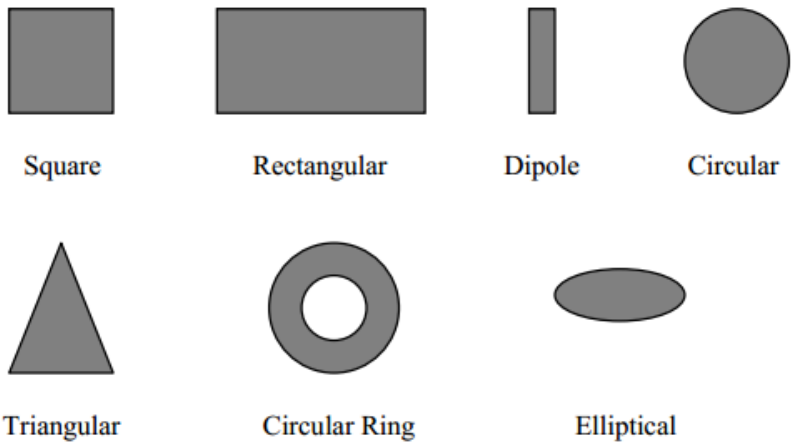

Figure 3.2: Different shapes of misrostrip patch element [13]

3.2 Advantages and Disadvantages

Microstrip patch antennas have many advantages when compared to all non-planar antennas. Because of this, they are increasing in popularity and have usage in wide range of applications like mobile and compact devices, wireless communication, cellular phones, aircraft and satellite communications. Antennas for these types of applications need to be thin and compact. Some of the principal advantages of patch antennas discussed by authors [13, 17] are given below:

- Light weight and low volume
- Can be fabricated in large quantities due to low fabrication cost
- Low profile planar arrangement that can be easily mounted on any type of surface
- Operate at both linear as well as circular polarization
- Capable of resonating at dual and triple frequencies

- Easy integration with microwave integrated circuits (MICs)
- Mechanically robust when mounted on rigid surfaces

Despite several advantages, microstrip patch antenna suffers from various weaknesses as compared to conventional antennas. Some of the important disadvantages discussed in [17, 18] are given below:

- Narrow bandwidth
- Low Gain
- Low efficiency
- Poor end fire radiator except tapered slot antennas
- Extraneous radiation from feeds and junctions
- Low power handling capacity.
- Surface wave excitation

The frequency bandwidth of a microstrip patch antenna is only a fraction of its operating frequency. Spurious feed radiation often appears. They also have high Q factor. The Q factor shows the losses associated with an antenna it is the main cause of narrow bandwidth.

3.3 Antenna Feeding Techniques

Several feeding technique are available for different types of microstrip patch antenna. They are divided into two categories: contacting and non-contacting [13]. In contacting feed method, as the name suggests, the RF power is fed directly to the patch element by physical contact through a microstrip line. While in non-contacting, the power transfer between microstrip line and patch element is achieved through electromagnetic field coupling. Four widely used feed methods are microstrip line, coaxial probe (both contacting feed), aperture coupling and proximity coupling (both non-contacting feeds).

3.3.1 Microstrip Line Feed

In this feeding method, a conducting strip and the patch element are connected edge-to-edge, as shown in Fig. 3.3. Microstrip feed line is a conducting strip of much smaller width than the patch element. The advantage of this type of feed is that the strip can be etched on the substrate to make a planar structure.

The strip is easy to fabricate and simple to match by controlling its width and inset position. The purpose of the inset cut is to match the impedance of microstrip with that of the patch element without any other matching element. However, with the increase in substrate thickness, spurious radiation and surface waves also increase which limits the bandwidth of the patch antenna. The feed radiation also creates undesired cross polarization.

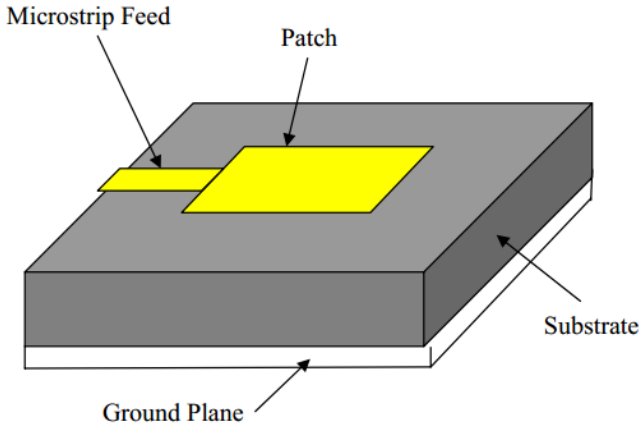

Figure 3.3: Microstrip line feed [11]

3.3.2 Coaxial Feed

The coaxial feed, also known as probe feed, is a widely used feeding technique to feed microstrip patch antennas. As shown in Fig. 3.4, the RF power is transferred through the inner conductor of coaxial cable which is soldered to the patch element through a hole in the substrate. The outer conductor is connected to the ground plane.

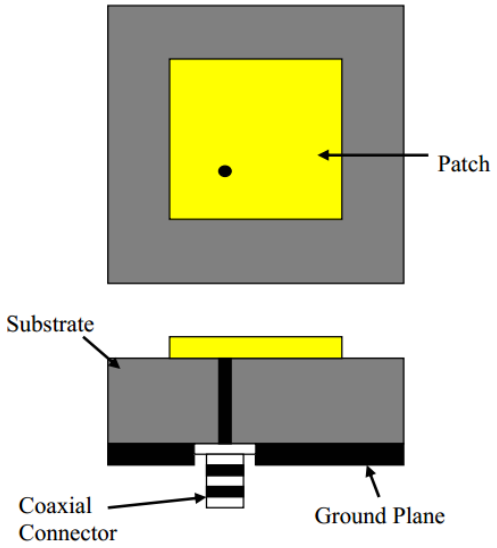

Figure 3.4: Coaxial fed microstrip patch antenna [11]

The coaxial feed is easy to fabricate and has very low spurious radiation than microstrip line feed. The coaxial probe is easy to place over any desired point on the patch element in order to match the input impedance. However, the coaxial feed provides narrow bandwidth which is its major disadvantage. Also, it is difficult to model because it requires a hole to be drilled in the substrate. The connector sticks out outside the ground plane, as seen in Fig. 3.4, which does not make antenna completely planar. The probe length makes feed inductive which leads to mismatch [17]. This problem is worse when thick substrates ($h>>0.02\lambda_0$) are used.

It is clear that despite ease of design and fabrication both of the contacting feed methods suffer from various disadvantages. The two non-contacting feed methods, discussed below, solve many of these problems.

3.3.3 Aperture Coupled Feed

In aperture coupled feeding, there are two substrates separated by a ground plane. On the bottom side of lower substrate there is a microstrip feed line which couples energy to the patch element through a slot or an aperture in the ground plane that separates the two substrates. The feed arrangement is shown in Fig. 3.5.

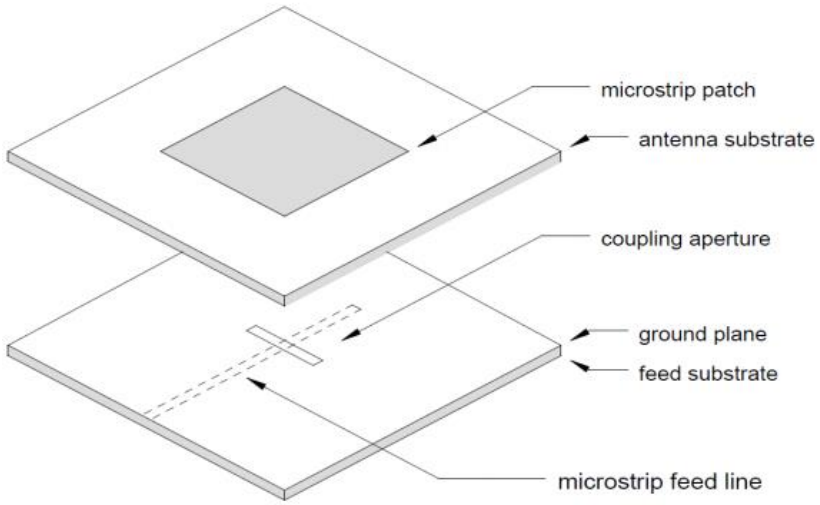

Figure 3.5: Aperture coupled feed [11]

This feed method provides independent optimization of the feed mechanism and patch element. The coupling slot is centered under the patch, leading to cross polarization due to symmetry of the arrangement. The shape, size and location of the slot determine the amount

of coupling from feed line to patch. The separation between ground plane and patch minimizes the spurious radiation. Usually, a thick and low dielectric constant material is used for the upper substrate and a substrate with high dielectric constant is used to optimize the radiation from the patch [13]. This feed configuration is difficult to fabricate, multiple layers increase antenna thickness and provides narrow bandwidth.

3.3.4 Proximity Coupled Feed

In proximity coupled feed, two dielectric substrates are used in an arrangement that feed line is sandwiched between two substrates and the patch element is on top of the upper substrate. The ground plane lays at the bottom the lower substrate, as shown in Fig. 3.6. This type of feeding is also known as electromagnetic coupling scheme.

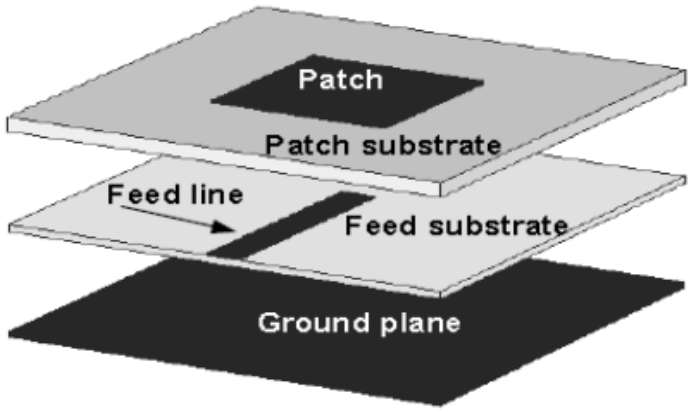

Figure 3.6: Proximity Coupled Feed [12]

Compared to other three feed models, proximity coupled feed offers high bandwidth (up to 13%) and very low spurious radiation. This feed offers individual substrate choice for patch element and feed line to optimize the individual performance. The impedance matching is done by controlling the length of the feed line and width-to-line ratio of the patch. The major disadvantages are difficult fabrication due to complex structure and increase in overall thickness of the antenna.

3.4 Patch Antenna Design using Transmission Line Model

In this section, the design procedure for a rectangular microstrip patch antenna using transmission line method is discussed. The transmission line model is a method for the analysis of microstrip patch antenna and field distribution of all TM_{00n} modes. The model is not accurate

but is simple and gives relatively good physical understanding of nature of a microstrip patch antenna.

This model represents a rectangular patch as a parallel-plate transmission line connecting two radiating slots or apertures each of width *W* and height *h*, as shown in Fig. 3.7. In Fig. 3.7, *z* is the direction of propagation of transmission line. The microstrip is a nonhomogeneous line of two dielectrics; substrate and air. The two slots represent high impedance termination (open-circuit) on both sides of transmission line. Therefore, depending on it length L, this structure have highly resonant characteristics.

In Fig. 3.7, it is shown that most of the field lines reside inside the substrate with some lines outside the patch in air. The transmission line cannot support pure transverse electro-magnetic (TEM) mode of transmission because phase velocities are different in substrate and

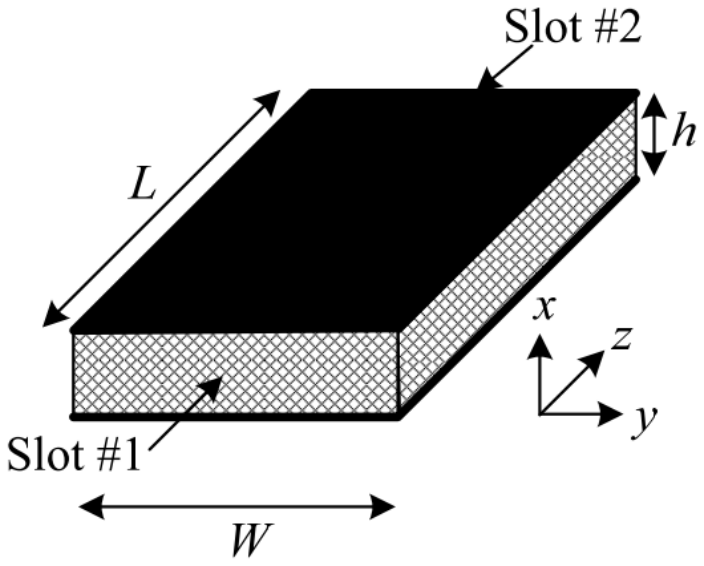

Figure 3.7: Transmission line model of rectangular microstrip patch antenna [11]

air. So, the mode of propagation in this case would be quasi-TEM mode. The quasi-TEM mode occurs when the phase velocity of the EM wave is not constant because of two different mediums (air and substrate in this case). Hence, effective dielectric constant, ε_{reff}, must be considered in order to account for the fringing fields. The fringing fields are not completely confined inside the substrate but are also spread in air. Hence, the value ε_{reff}, of is slightly less than ε_r, and is given by Balanis [19] as:

$$\varepsilon_{reff} = \frac{\varepsilon_r+1}{2} + \frac{\varepsilon_r-1}{2}\left[1+12\frac{h}{w}\right]^{0.5} \quad (3.1)$$

Where ε_{reff} = effective dielectric constant

ε_r = dielectric constant of substrate

h= height of dielectric substrate

W= width of the patch

For antenna to operate in fundamental TM_{10} mode, the length of patch element should be slightly less that *λ/2*, where λ is wavelength in dielectric medium and is given as $\lambda_0 / \sqrt{\varepsilon_{reff}}$ and λ_0 is wavelength in air. The TM10 mode implies that the field varies *λ/2* cycle along patch length and no variation occurs along patch width.

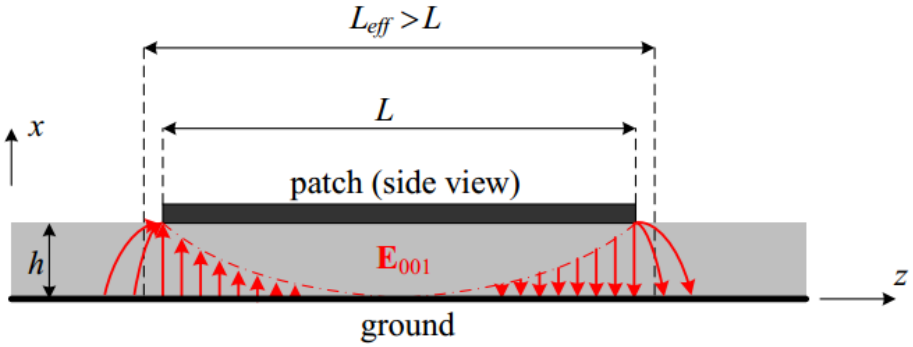

Figure 3.8: Effect of fringing fields on length of patch element [11]

Figure 3.8 shows that because of fringing fields, the resonant length of patch is not equal to the physical length *L*. The dimensions of path on each end along its length have been increased by distance *ΔL,* thus $L_{eff} > L$. Whereas, *ΔL* is given by Hammerstad [20]as:

$$\Delta L = 0.412h \frac{\left(\varepsilon_{reff}+0.3\right)\left(\frac{W}{h}+0.264\right)}{\left(\varepsilon_{reff}-0.258\right)\left(\frac{W}{h}+0.8\right)} \tag{3.2}$$

The effective length of the patch L_{eff} becomes:

$$L_{eff} = L + 2\Delta L\, W \tag{3.3}$$

For a given resonance frequency f_0, the effective L_{eff} length is given by [17] as:

$$L = \frac{c}{2f_0\sqrt{\varepsilon_{reff}}} \tag{3.4}$$

The resonant frequency f_0 rectangular microstrip patch antenna at any TM_{nm} mode is given by James and Hall [21] as:

$$f_0 = \frac{c}{2f_0\sqrt{\varepsilon_{reff}}}\left[\left(\frac{m}{L}\right)^2 + \left(\frac{n}{W}\right)^2\right]^{\frac{1}{2}} \quad (3.5)$$

where *m* and *n* are modes along *L* and *W* respectively.

The patch width *W* is given by Bahl and Bhartia [22] as:

$$W = \frac{c}{2f_0\sqrt{\frac{(\varepsilon_r+1)}{2}}} \quad (3.6)$$

Theoretically, the patch antenna designing using transmission line method requires an infinite ground plane. But for practical applications, it is impossible to achieve an infinite ground plane. However, it has been proved by the research [17] that similar results can be achieved with a finite ground plane if its size is greater than the patch size by six times the substrate thickness in all dimensions. Hence, the formulas for the ground plane dimensions can be written as:

$$L_g = 6h + L \quad (3.7)$$

$$W_g = 6h + W \quad (3.7)$$

Where L_g=lebgth of groud plane

W_g = width of ground plane

Chapter 4

U-Slot Microstrip Patch Antenna

In this chapter, an introduction to U-slot microstrip patch antenna is given along with its advantages. The purpose introducing this antenna and its development background and evolution are also discussed. After that, two design approaches are discussed and detailed design method is presented. In order to understand the behavior of antenna, some parametric studies are performed. Finally, the tuning steps are given to achieve the dual-band and wide-band antenna characteristics.

4.1 Introduction

The rapid development and evolution of high-speed wireless communication in recent years along with the increasing necessity of high-performance mobile applications have led to extensive research into broad-band and low profile antennas. The physical characteristics of microstrip patch antennas make them ideal for mobile devices, wireless local networks, Bluetooth and other compact devices. Such characteristics are also required for aperstructure and opportunistic array concepts.

The traditional rectangular microstrip patch antennas (discussed in the previous chapter) hardly provide bandwidth of up to 2% [21]-[23], which is too narrow to support wireless communication systems discussed above. On the other hand, such applications also require multi-band antennas for devices to operate on multiple frequency bands to provide application diversity. A rectangular microstrip patch antenna is not suitable to be utilized for such systems because it usually has a single resonant frequency f_r [18]. However, the rectangular microstrip patch antenna can be modified in a way that it can operate at dual or multiple frequency bands with increased bandwidth [17].

Several techniques for increasing the bandwidth of microstrip patch antenna have been developed. Two of the most common and simplest techniques are increasing the substrate height and decreasing the dielectric constant [13, 17-19]. However, by increasing substrate height, the patch size increases (which nullifies the low-profile property of the patch) and the substrates with lower dielectric constants are very hard to design [18]. Other complex techniques include a stacked patch (multilayer configuration of several parasitic elements above the driven element) and a coplanar parasitic sub-array (planar structured patch antenna bounded by closely spaced parasitic patch elements). However, the low-profile and antenna compactness cannot be achieved with these methods [13]. Other technique involves aperture

coupled excitation. But, as discussed in section 3.4.3, the fabrication of this type of configuration is complicated due to the complex feeding.

The patch antenna bandwidth can also be increased by modifying the basic geometry of the antenna while maintaining the low-profile and compactness. Some of such configurations [24] are shown in Fig. 4.1 that provide increased bandwidth. However, the analysis of these patch antennas is complex. The complex shape makes it difficult to analytically represent the relationship between antenna geometries and characteristics.

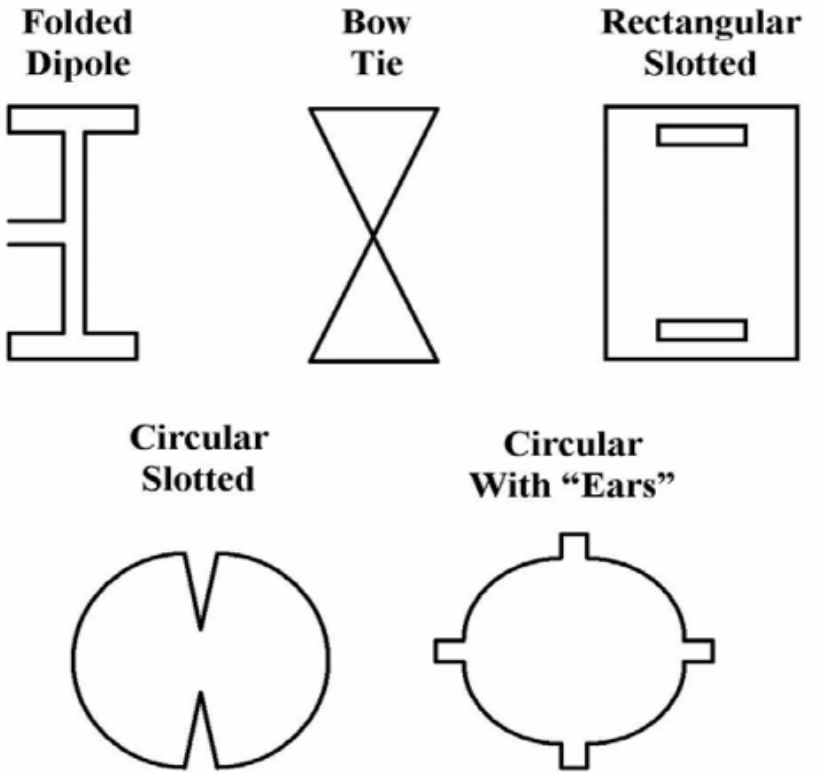

Figure 4.1: Some high bandwidth microstrip patch antennas [10]

The most convenient method to achieve multi-band microstrip patch antenna along with increased bandwidth is by introducing slots to the patches. A simple rectangular patch antenna typically resonates at a single resonance frequency f_r. It can be modified to resonate at multiple frequencies by including slots [25] of different shapes into it. Several different types have been reported which include mainly C, E, F and U slot shapes each one with its own effects and properties. The slot antenna performance strongly depends on the shape and position of the slot and multiple slots can be included to obtain the desirable performance [13, 25].

The form of slotted rectangular microstrip patch antenna selected for this project is known as U-slot microstrip patch antenna. This type of antenna is easy to design and provides increased bandwidth with dual- and/or multi-band operations. Its design and properties are discussed in great detail in following sections.

4.2 U-Slot Microstrip Patch Antenna

The first patch antenna with U-slot was reported by Huynh *et al.* [26] in 1995 fed by a probe with air as dielectric medium between patch and ground plane. The antenna showed wideband characteristics and provided an impedance bandwidth of 47% which was quite good because simple patch antenna hardly provides bandwidth of up to 2% [26]. This was a pioneering design because it achieved large bandwidth with a simple topology by using a U-slotted patch, coaxial feed and a single layer foam substrate. Since then, many practical and theoretical studies have been carried to know about the relationship between antenna design and its behavior and to develop analytical design procedure. The authors [26] claimed that the wideband antenna behavior was due to the current along the edges of the slot that produce another resonance which combine with the resonance of the main patch. In [27], the authors showed that U-slot patch antenna maintains its wideband characteristics with linear polarization when fabricated on a microwave substrate instead of an air or foam substrate. Previously, the U-slot was considered as a mean to achieve only wideband antenna behavior rather than multiband resonances. Later on, the researchers [28] showed that by varying some U-slot parameters the wideband antenna can be converted into a dual-band antenna.

Subsequently, the researchers in [28, 29] revealed even more important fact that when cutting more than one U-slot on the patch, the antenna can resonate at multiple frequencies. The U-slots introduce notches [28] into the wideband of antenna, resulting multiband operation. Such extraordinary findings increased the range of applications for U-slot patch antennas from wideband to multiband operation. Along with these characteristics, the antenna polarization can also be changed by manipulating the U-slot. Because of these properties and due to its simple geometry, the U-slot patch antenna can be customized to be used for numerous small-scale and multiband devices.

The geometry of a simple coaxial-fed rectangular microstrip patch antenna with a U-slot is shown in Fig. 4.2 (a). The length and width of patch antenna are represented by *L* and *W*, respectively. The U-slot has two vertical arms, each of length *C*, and a width of length *D*. The widths of horizontal and vertical slots are E and *F*, respectively. y_P shows the vertical distance of feed point from the center of the rectangular patch. The feeding method by a coaxial probe is shown in Fig. 4.2 (b). Inner conductor of coaxial probe is attached with patch at point *P* through a hole and its outer conductor is attached with the ground plane of the substrate.

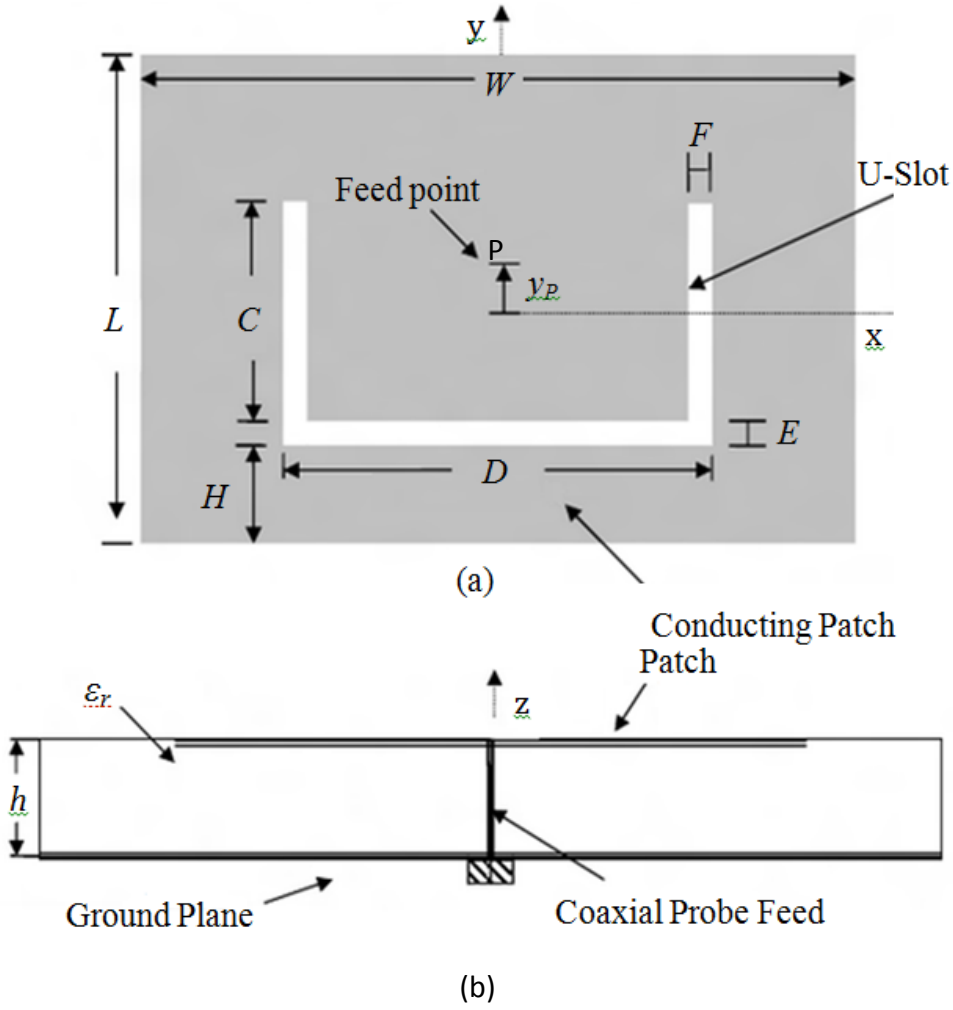

Figure 4.2: (a) Geometry of a rectangular U-slot microstrip patch antenna (b) Coaxial probe feeding method [30]

4.3 U-Slot Microstrip Patch Antenna Design Approaches

It has been shown experimentally that antenna behavior can be affected by variation in parameters like size of the patch element, width *D* and length *C* of the U-slot, height *h* and substrate permittivity ε_r and feed point. Since the introduction of U-slot microstrip patch antenna in 1995 [26], researchers have attempted to formulate the design procedure for the antenna based on the experimental studies. But, no specific analytical model has been developed until now [30]. However, two different analytical design methods have been introduced by researchers in [31, 32]. The two design approaches yield significantly different antenna designs. However, they provide a good starting point to design a U-slot microstrip patch antenna.

Researchers [33, 34] have attempted to compare the U-slot patch antenna design procedures presented in [31, 32]. It is worth mentioning that both the methods require significant tuning to achieve broad-band and/or dual-band operation. The measure of performance may be the number of optimization cycles needed to achieve the required antenna characteristics. In the following subsections, the concepts, limitations and advantages of both the procedures are discussed.

4.3.1 Dimensional Invariance Design Approach

The design procedure proposed in [31] is based on dimensional invariance relationships observed between U-slot geometry and empirical design equations. The empirical formulas given in this paper are for U-slot patch antenna operating in frequencies ranging from 2GHz to 6GHz. The advantage of this method is that when the desired frequency lies between this range, the design procedure converges the optimized design quickly. However, it may provide some reasonable design parameters for antenna operating outside the mentioned frequency range. The disadvantage of this method is that the equations are derived for specific values of dielectric constant ε_r and height h of the substrate. It limits the usefulness of this methoid because it does not give desired antenna performance for all possible combinations of ε_r and h.

The fact that this method appears to generate initial antenna designs that have good agreement with the intended response for particular frequency range, in which our desired frequencies (2.1GHz and 3.5GHz) reside, this method was given priority. On the other hand, the authors in [31] also suggest some fine-tuning procedures to obtain a wide-band and/or dual-band antenna operations.

4.3.2 Resonance Frequency Design Approach

The second method to obtain design parameters for U-slot microstrip patch antenna is proposed in [32]. The method assumes the existence of four different resonant frequencies to determine the dimensions of the U-slot. It keeps the VSWR at resonant frequencies as close as possible to balance the tradeoff between bandwidth and VSWR. It also tries to achieve a constant VSWR over the desired resonant frequencies. Ultimately, the resulting impedance loop is centered at the center of Smith chart. The design equations in this method are based on the theory of rectangular microstrip patch antenna, not U-slot patch antenna. The resulting antenna design, however, has results close to the desired frequencies.

This method suffers from three major weaknesses. First, the studies were performed only for substrates with low permittivity. The authors did not provide the applicability of the

design equations to medium and high permittivity substrates. Second, the design equations may yield antenna parameters that are physically unfeasible. Third, the tuning procedure requires much more iterations as compared to dimensional invariance design approach to optimize the design.

4.4 Initial Design Procedure

In this thesis, the dimensional invariance design procedure given in [31] is used to get the initial parameters for desired U-slot microstrip patch antenna. The procedure may not produce an antenna working exactly on desired frequencies. Therefore, the optimization must be done to fine-tune the antenna. Several tuning methods have been proposed in [31, 33-34] to achieve the broad-band and dual-band operation. The design steps given in [31] are as follows:

1. Identify the desired antenna resonant frequency and 2:1 VSWR bandwidth.
2. Approximate the resonant frequency as f_{res3} and the upper and lower frequency bounds of the bandwidth as f_{res2} and f_{res4} respectively.

3. Select a substrate permittivity ε_r and a substrate thickness h.

4. Broad-band operation is not possible due to lower limit on h. Therefore, the substrate parameter h and ε_r should satisfy the following equation [27, 35]:

$$h \geq 0.06 \frac{\lambda_{0res3}}{\sqrt{\varepsilon_r}} \tag{4.1}$$

where λ_{03res} = wavelength at the resonant frequency in air.

5. Quantity estimation of ($L + 2\Delta L$):

$$L + 2\Delta L = \frac{c}{2\sqrt{\varepsilon_r} f_{res3}} \tag{4.2}$$

where c= speed of light in free space.

6. Calculate W as

$$W = 1.5(L + 2\Delta L) \tag{4.3}$$

7. Calculate the effective permittivity, ε_{eff}, and $2\Delta L$ using:

$$\varepsilon_{reff} = \frac{\varepsilon_r + 1}{2} + \frac{\varepsilon_r - 1}{2} \left[1 + 12 \frac{h}{w}\right]^{-\frac{1}{2}} \tag{4.4}$$

$$2\Delta L = 0.824h\frac{\left(\varepsilon_{reff}+0.3\right)\left(\frac{W}{h}+0.264\right)}{\left(\varepsilon_{reff}-0.258\right)\left(\frac{W}{h}+0.813\right)} \quad (4.5)$$

8. Calculate *L:*

$$L = \frac{c}{2\sqrt{\varepsilon_r}\, f_{res3}} - 2\Delta L \quad (4.6)$$

9. Calculate U-slot thickness:

$$E = F = \frac{\lambda_{0res3}}{60} \quad (4.7)$$

10. Compute *D*

$$D = \frac{c}{\sqrt{\varepsilon_r} f_{res2}} - 2(L + 2\Delta L - E) \quad (4.8)$$

11. The value of C should satisfy below equations:

$$\frac{C}{W} \geq 0.3 \quad (4.9)$$

$$\frac{C}{D} \geq 0.75 \quad (4.10)$$

12. Calculate $\varepsilon_{eff(pp)}$ and effective length of pseudo-patch:

$$\varepsilon_{eff(pp)} = \frac{\varepsilon_r+1}{2} + \frac{\varepsilon_r-1}{2}\left[1+\frac{12h}{D-2F}\right]^{-\frac{1}{2}} \quad (4.11)$$

$$2\Delta_{L-E-H} = 0.824h\,\frac{\left(\varepsilon_{reff(pp)}+0.3\right)\left(\frac{D-2F}{h}+0.264\right)}{\left(\varepsilon_{reff(pp)}-0.258\right)\left(\frac{D-2F}{h}+0.813\right)} \quad (4.12)$$

13. Calculate *H* by

$$H \cong L - E + 2\Delta_{L-E-H} - \frac{1}{\sqrt{\varepsilon_{eff(pp)}}}\left[\frac{c}{f_{res4}} - (2C + D)\right] \quad (4.13)$$

14. The sum of slot arm, slot width and H (*C + E + H*) should be less than *L*. Otherwise, recalculate the in C (step-11) by changing the ratios.

After going through all these design steps, the design parameters for U-slot microstrip patch antenna are obtained which will operate at frequencies near the defined resonant frequencies. Therefore, optimization must be done to get the exact results.

4.5 Optimization

In order to perform tuning, it is required to understand the relationship between the geometry of U-slot patch and its impedance characteristics. In practice, the parameters which control the size and location of input impedance are considered as important for tuning process. Authors in [32] investigated the effect of U-slot geometry on the impedance characteristics to form an optimization method. In this section, these characteristics are discussed in detail in next sub-section.

4.5.1 Bandwidth Characterization on Smith Chart

The nature of the antenna performance can be studied from the impedance loop on Smith chart. In Fig. 4.3 four general forms of impedance loci, numbered 1 to 4, on a Smith chart are shown. Each of the four loops represents a frequency sweep (from f_{min} to f_{max}). For an ideal performance, the impedance loop should converge to the center point (*VSWR = 1*) of the Smith chart. More the loop encircles the center, higher the antenna bandwidth is achieved. Such a loop is loop 4 in Fig. 4.3. Rest of the loops will give a distorted antenna performance, which is discussed later in this section. For practical applications, the location and size of the loop is required to be such that *VSWR ≤ 2*, which corresponds to a return loss of -10dB or lower [20-22].

From Fig. 4.3, it can be noticed that the task of achieving dual-band and broadband antenna performance lies in examining how the dimensions of the U-slot patch antenna affect the movement of impedance locus on Smith chart. The researchers in [32] performed this by changing one dimension of antenna, keeping others unchanged, and recording the resulting changes on loop. These are (1) substrate thickness h (2) probe location y_P (3) slot width E and F (4) ratio of distances between U-slot and upper edge and lower edge of the patch $\frac{G}{H}$ and (5) probe radius. The effect of each of these dimensions is presented below. Although, these studies are not exhaustive, but they provide a good start pointing point for antenna tuning.

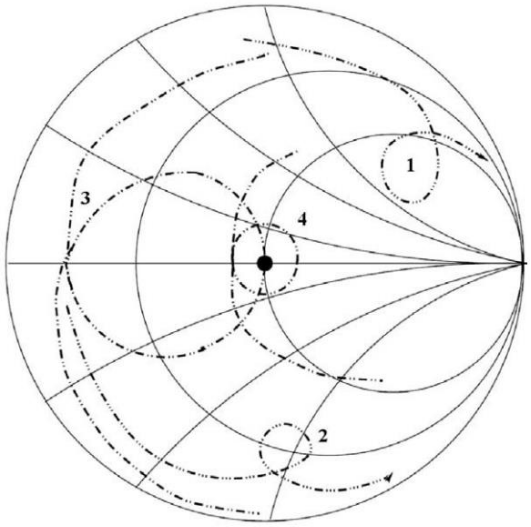

Figure 4.3 General impedance loci for U-slot microstrip patch antenna [30]

1. Effect of Substrate Height (*h*)

   The effect of varying substrate height *h* on the impedance loop of U-slot patch is shown in Fig. 5.4. It can be noticed that increase in height makes the impedance loop to shrink and move towards the center of Smith chart, which suggests increase in bandwidth. Also, the impedance becomes more capacitive because the loop shifts down towards the capacitive part of the Smith chart.

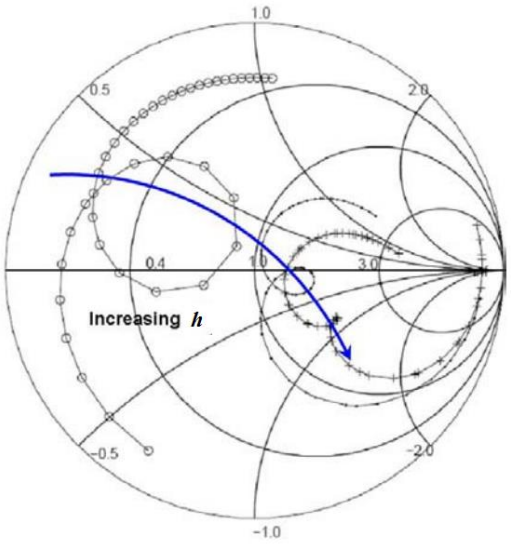

Figure 4.4 Effects of substrate height on impedance loop [30]

2. Effect of Probe Location (y_P)

   The effects on varying probe location y_P on the impedance loop are shown in Fig. 5.5. The studies performed in [32] show the size of the impedance loop decreases and it becomes more inductive when the probe (feed point) is moved in positive direction along y-axis. The inductive behavior in impedance is obtained because the loop shifts towards the upper half of the Smith chart which is inductive. On the other hand, it is also reported that dual-band antenna behavior can be obtained by shifting probe on positive and negative x-axis.

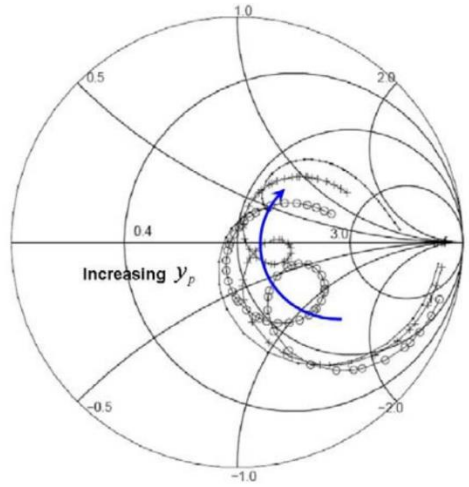

Figure 4.5 Effects of probe location on impedance loop [30]

3. Effect of Slot Width (*E* and *F*)

   The effects of changing size of slot widths *E* and *F* on performance of U-slot microstrip patch antenna are shown in Fig. 5.6. The impedance loop decreases in size and become more inductive if slot width is decreased. It also has effect on dual-band behaviors of antenna because the difference between the two frequencies is reduced when width is increased and vice versa. Hence, desired frequencies can be achieved by effectively varying *E* and *F*.

4. Effect of ratio $(\frac{G}{H})$

   The effect of varying the $(\frac{G}{H})$ ratio on the impedance loop is shown in Fig. 5.7. The studies show that with increase in $(\frac{G}{H})$ ratio, the impedance behavior slightly becomes inductive and loop becomes decreasing in size. This suggests that the bandwidth of antenna will increase if the ratio is increased.

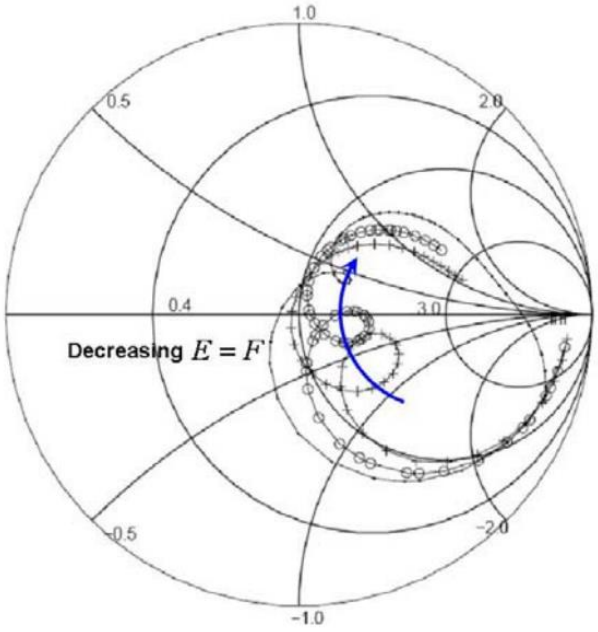

Figure 4.6 Effect of U-slot width on impedance loop [30]

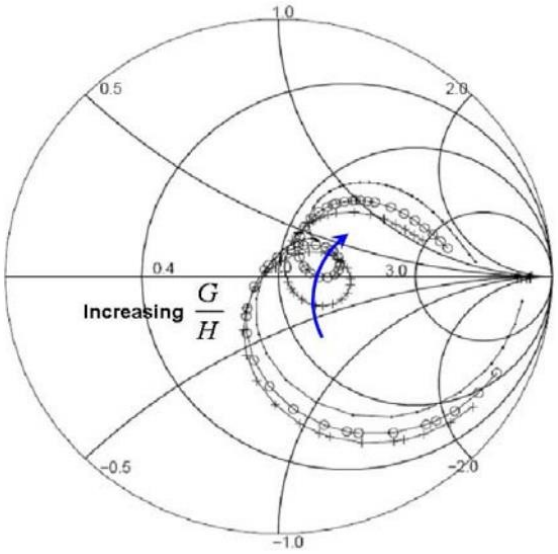

Figure 4.7 Effect of $\frac{G}{H}$ ratio on impedance loop [30]

5. Effect of Probe Radius (r_{inner})

   The parametric studies show that variation in probe radius r_{inner} does not alter the size of the impedance loop. However, the nature of the impedance becomes

inductive when the radius size is decreased. The effects of probe radius on impedance loop are shown in Fig. 5.8.

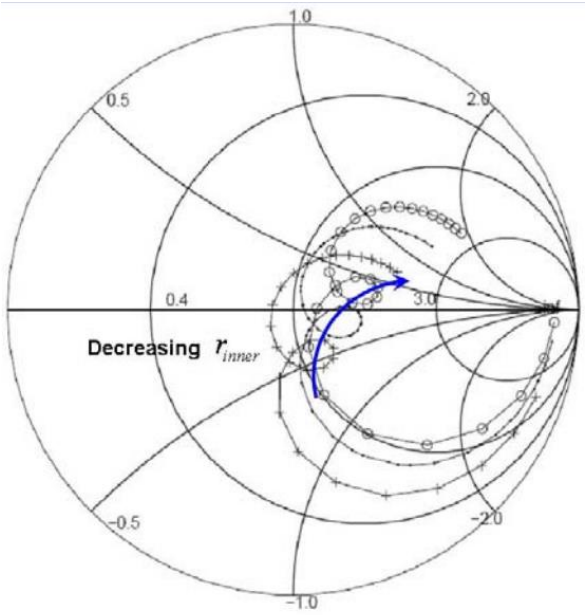

Figure 4.8 Effects of probe radius on impedance loop [30]

4.5.2 Tuning Techniques

In this section, the steps for optimizing the initially designed U-slot microstrip patch antenna are recommended to achieve dual-band and wide-band antenna operation. These steps are derived after performing the parametrical studies and observing the effect of each parameter of antenna performance, as mentioned above, and can be used to quickly tune the antenna to the required performance.

1. Vary the substrate thickness, *h*, slot width, *E* and *F*, as well as probe location, y_P, in positive y and x-axes, so that the size of the impedance loop can be reduced and it can encircle the center (*VSWR = 1*) point of the Smith Chart.

2. If the size of the impedance loop is very large, increase the ratio $(\frac{G}{H})$ to reduce the loop size while minimizing the effect on its location.

3. If necessary and possible, vary the probe radius, r_{inner}, as a method to refine the size and location of the impedance loop.

Chapter 5

Antenna Design and Simulation Results

5.1 Initially Designed Single Element Patch Antenna

Substrate selection is the first practical step in designing a patch antenna. For this project, Rogers TMM3 [36] high frequency laminate was initially selected as substrate to design the patch antenna. The dielectric constant and height values chosen for the substrate are ε_r = 3.27 and h = 6.35mm, respectively. These values are carefully selected to meet our performance and bandwidth requirement because dielectric material is crucial for determining the performance of antenna. To achieve compactness, thin substrates are required but the bandwidth of patch antenna decreases as height is reduced [21]. Also with higher values of ε_r the patch size can be reduced but it would also reduce the antenna bandwidth [18]. So, a trade-off must be done between antenna performance and its size.

The empirical formulas presented in chapter 4 (section 4.5.1) of chapter 4 are used here to obtain the initial parameters of dual band U-slot patch antenna. The inputs to these formulas are the values of ε_r, h and desired frequencies. A MATLAB code is written to calculate values of antenna parameters for different values of ε_r, h and operating frequencies. This generic code will help avoid repetitive manual calculations and will instantly provide all required antenna parameters. The code is given below.

```
f0 = 2.05*10^9;

flow = 1.6*10^9;

fhigh = 2.6*10^9;

v = 3*10^8;

Er = 3.27;

h = 0.00635;

lambda = v/f0;

hh =(0.06*lambda)/sqrt(Er)  %required substrate height

%W = (v/(2*f0))*sqrt(2/(Er+1));

W=1.5*(v/(2*sqrt(Er)*f0));
```

```
Ereff = (Er+1)/2 + ((Er-1)/2)*(1+12*h/W)^(-0.5);

Leff = v/(2*f0*sqrt(Ereff));

deltaL = 0.412*h*(Ereff+0.3)*(W/h+0.262)/(Ereff-0.258)/(W/h+0.813);

L = Leff - 2*deltaL;

E = lambda/60;

F = lambda/60;

D = v/(flow*sqrt(Ereff)) - 2*(L+(2*deltaL)-E);

C1 = 0.3*W;

C2 = 0.75*D;

Ereffpp = (Er+1)/2 + ((Er-1)/2)*((1+12*h/(D-2*F))^(-0.5));

deltaLEH    =    0.412*h*(Ereffpp+0.3)*((D-2*F)/h+0.262)/(Ereffpp-0.258)/((D-
2*F)/h+0.813);

C=C1;

H = L - E + (2*deltaLEH) - (1/sqrt(Ereffpp))*(v/fhigh-(2*C+D));

Checksum = C + E + H;
```

Table 5.1 shows the U-slot microstrip patch antenna parameters obtained from the above MATLAB code. These initial parameters provide good approximate results at first attempt. Then, parametric tuning was performed in ADS Momentum to get desired antenna performance. To feed the antenna a coaxial probe of characteristic impedance 50Ω is used. The coaxial probe introduces inductance to the patch which is cancelled by U-slot [13].

Table 2: Initial dimensions of single element U-slot patch antenna

U-Slot Microstrip Patch Antenna							
W	L	C	D	E	F	H	y_P
60.7	37	18.2	29.1	2.4	2.4	10	0

Fig. 5.1 shows the layout of the initially designed (un-optimized) single element dual-band U-slot patch element, designed in Agilent ADS Momentum. The antenna is fed by a port at the center having characteristic impedance of 50Ω. During simulation process, the substrate losses are taken into consideration. The tangent loss for the selected substrate is 0.0009 [36].

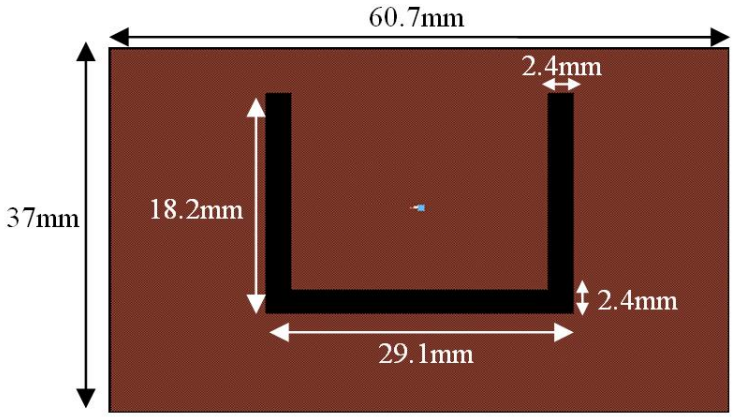

Figure 5.1: Layout of initially designed U-Slot patch antenna

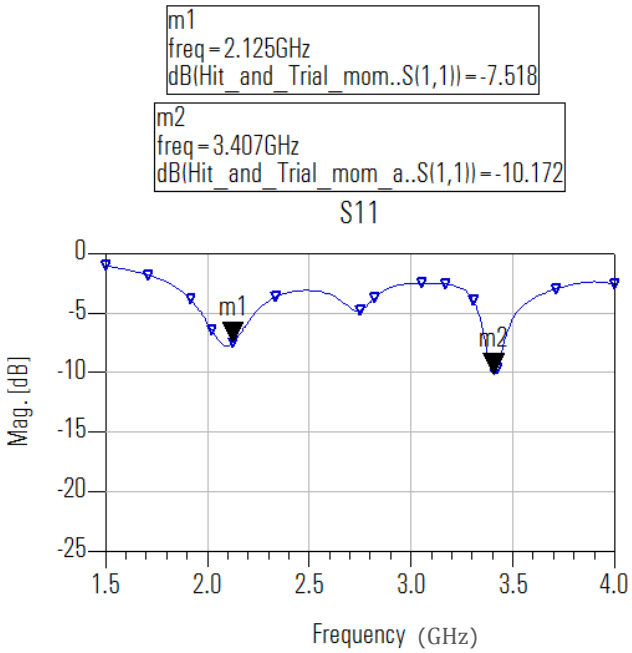

Figure 5.2: Initially designed patch antenna reflection coefficient – S_{11}

After designing the U-slot patch antenna, it was simulated to check its performance and obtained frequencies. To analyze the antenna, the Agilent ADS helps us to get information about various parameters of antenna such as reflection coefficient, VSWR, directivity, gain, 2D and 3D radiation patterns, impedance loop plot on smith chart and current distribution. The reflection coefficient (S_{11}) plot of the un-optimized U-slot patch antenna is shown in Fig. 5.2. It is clear from the plot that result of the antenna parameters obtained using the formulas is not exact but there are some useful facts that can be further optimized to obtain intended antenna performance. The first fact is that the antenna resonates at two frequencies; 2.125GHz and

3.407GHz indicated by two markers named *m1* and *m2* on Fig. 5.2. Secondly, the two resonance frequencies of the antenna are near our desired frequencies. This design cannot be used for any practical purpose because the S_{11} for both frequencies is very low i.e. $VSWR \geq 2$. Fig. 5.3 shows the impedance loop plot of the un-optimized U-slot patch antenna. In the Fig. 5.3, two loops can be observed, which also confirms that the antenna resonates at two frequencies. It can be seen that the size of the first loop is very large. According to the studies presented in previous chapter, this indicates that the impedance of the coaxial probe and patch element are mismatched. The second loop is much smaller in size, however, it is well displaced from the center of the chart. This indicates that the bandwidth for the second frequency is very low.

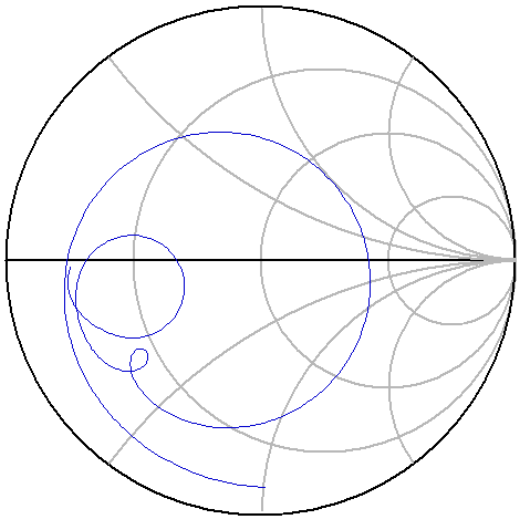

Figure 5.3: Impedance loop plot of initially designed patch on Smith chart

As claimed by the authors in [32], the design formulas give approximate antenna design parameters. These parameters can serve as a good starting point to achieve the desired antenna performance. In the following section, the optimized antenna is presented along with its results.

5.2 Optimized Single Element Patch Antenna

In this section, the simulation results of an optimized single element U-slot microstrip patch antenna are presented. The tuning process presented in chapter 4 is used to optimize the initially designed antenna to achieve the desired performance. Each of the steps was done one by one and its effect was observed on the antenna performance by making repeated

simulations. The principal steps involved moving the feed point in positive y-axis, changing the width of slot arms and decreasing the width of patch element. The antenna dimensions obtained after necessary tuning on single antenna element are shown below in Table 5.2.

Table 3: Dimensions of optimized single element U-slot patch antenna

U-Slot Microstrip Patch Antenna							
W	L	C	D	E	F	H	y_P
58	37	20	29	2.5	2.5	10	5

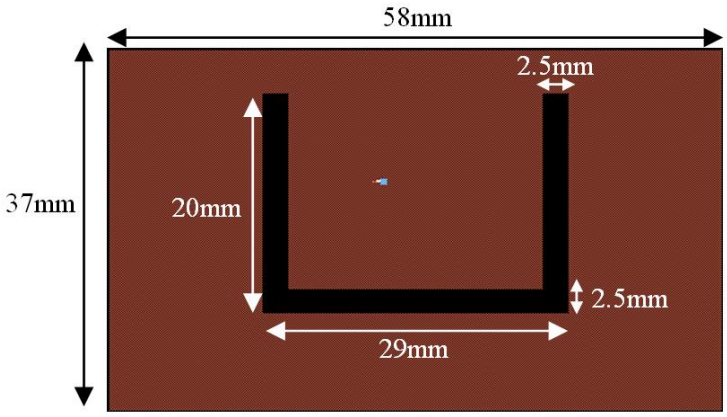

Figure 5.4: Layout of optimized U-Slot patch antenna

Fig. 5.4 shows the layout of optimized single element dual-band patch element, implemented in ADS Momentum. The reflection coefficient (S_{11}) or return loss plot of the above antenna is shown in Fig. 5.5. S_{11} at 2.1GHz and 3.5GHz is 22.24dB and 23.61dB respectively. These values of S_{11} at both the frequencies suggest that the antenna has good impedance matching. The 10dB bandwidth for 2.1GHz band comes out to be 90MHz and for 3.5GHz band it is 100MHz. The frequency bandwidth requirements for both the desired LTE bands, mentioned in chapter 1, are satisfied. The impedance loop plot of the optimized antenna is shown in Fig. 5.6. As compared to Fig. 5.3, the size of both of the loops is smaller. The impedance at the feed point for both the frequency bands is shown by markers *m1* and *m2*. The impedance values show good matching between feed point and coaxial probe. The loops do not encircle the center of the chart, which suggest that the bandwidth of the antenna is not high. However, the bandwidth achieved for both the frequency bands is enough to meet the requirements. Hence, there is no further need to optimize the antenna.

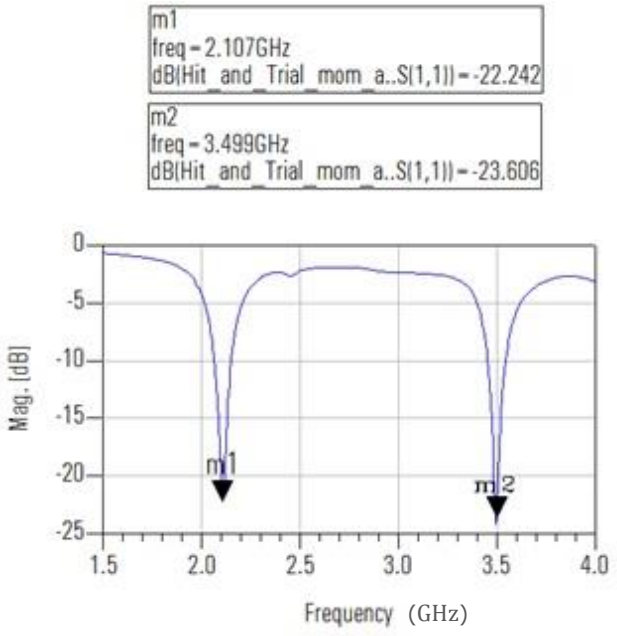

Figure 5.5: Optimized patch antenna reflection coefficient – S_{11}

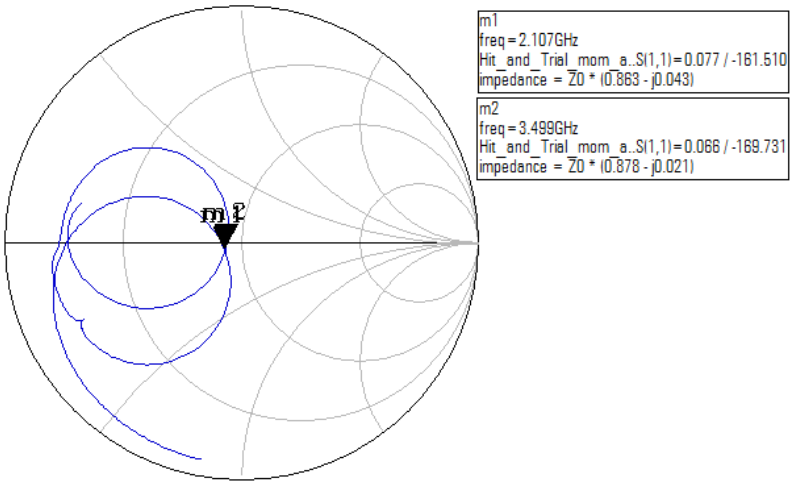

Figure 5.6: Impedance loop plot of optimized patch on Smith chart

Fig. 5.7 shows the antenna gain and directivity. Gain at 2.1GHz is above 7dBi. For 3.5GHz, the gain is found to be 5.7dBi. The antenna has an efficiency of 85% at 2.1GHz, as shown in Fig. 5.8. For 3.5GHz, it is found to be 75%. Fig. 5.9 shows the current distribution over the surface of U-slot patch element. The radiating edges are clearly identified. The current distribution shows that there are two radiations; one at the edges of rectangular patch and other around the

vertical arms of the U-slot. This confirms the basic theory of U-slot patch antenna that insertion of slot causes disturbance to current and triggers another radiation. The antenna resonates at 2.1GHz on the edges and at 3.5GHz around arms of U-slot.

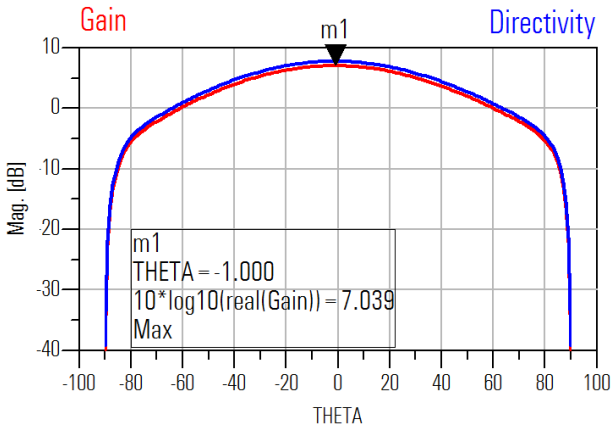

Figure 5.7: U-slot rectangular patch antenna single element antenna gain at 2.1GHz

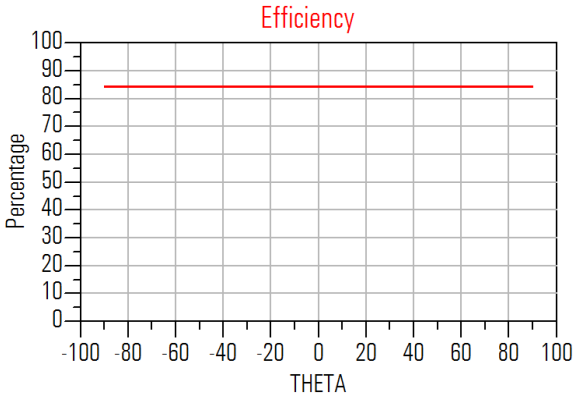

Figure 5.8: U-slot rectangular patch antenna single element efficiency at 2.1GHz

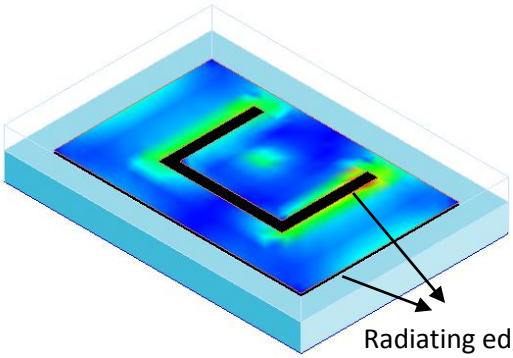

Figure 5.9: Surface current distribution on U-slot patch antenna

5.3 RF Anechoic Chamber

A radio frequency anechoic chamber is a shielded room made to absorb all of the reflections of electromagnetic waves. Its internal walls are covered by a material which absorbs the incident radiation. The environment of an anechoic chamber simulates an open space of infinite dimensions, hence creating a free space. Its origin comes from a concept of stealth aircraft that that absorbs or scatters the radar waves. It provides an ideal environment to perform antenna radiation pattern measurements, radar and electromagnetic interference tests.

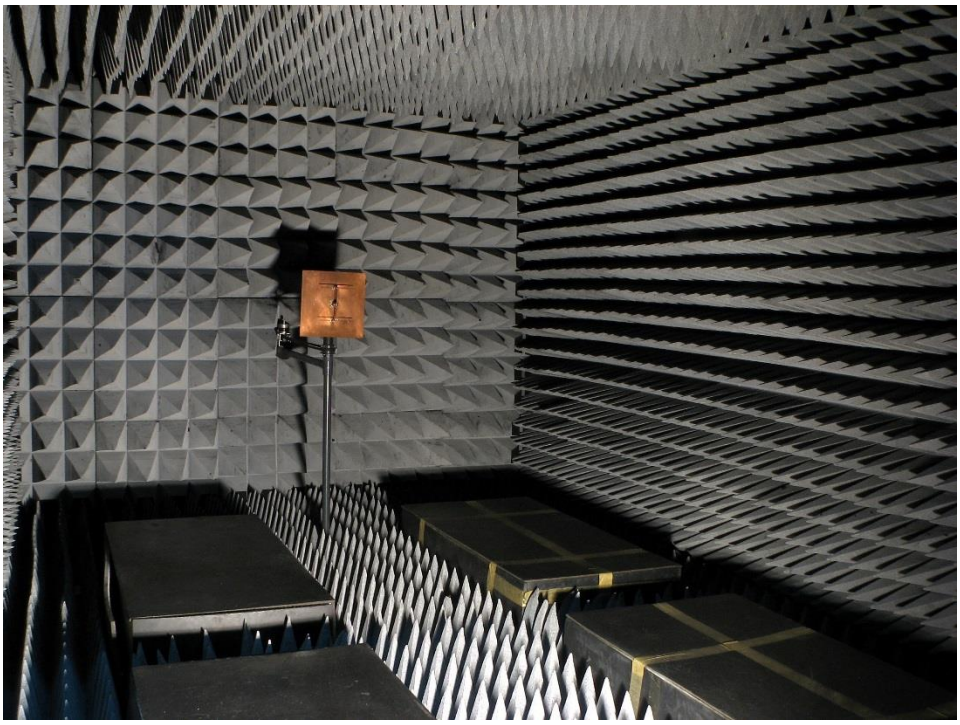

Figure 5.10: RF anechoic chamber [37]

The absorbent material inside the anechoic chamber is called radiation absorbent material or RAM. The RAM is designed to effectively absorb every possible incident RF radiation coming from every possible direction. More efficient is the RAM less will be the RF reflections. The spurious radiation and reflection are ensured to be negligible and all internal surfaces are covered with RAM to avoid any measurement errors and ambiguities. The most widely used and effective type of RAM is pyramid shaped, arranged in arrays. These are made from a highly lossy material. To install some equipment inside the chamber, sections of RAM can be removed but must be replaced to perform any tests. RAM is made of a rubber-type foam material which consists of mixture of carbon and iron. This material is neither a good conductor nor a good electrical insulator because neither of them absorbs energy.

Figure 5.11: Close view of Pyramidal RAM [37]

RAM can be considered as a transmission line. In order to design RAM, we must first know how to design a transmission line with zero reflection. The walls of the chamber are metallic, so the terminals of the transmission line will be short circuited. The pyramid shape of the RAM attenuated the incident waves by scattering and absorption. The scattering occurs in foam structure where carbon particles promote destructive interference. The pyramid shape is formed in a way that maximizes the number of bounces that incident wave makes within the material. The wave loses its energy at each bounce and apparently disappearing. The permeability and permittivity of RAM are complex which result in loss, as the wave pass through it. Usually, the RAM provides an attenuation rate of 11dB per centimeter [37].

5.4 RT/Duroid 5880 Antenna Simulation and Characterization

The antenna design presented in section 5.2 is not fabricated due to unavailability of the substrate and procurement problems. Because of this, RT/Duroid 5880 substrate was chosen as an alternate to TMM3. The dielectric constant and height values chosen for the substrate are ε_r = 2.2 and h = 3.175mm, respectively. The antenna was redesigned and remodeled according to the new substrate characteristics. For the new design, a compromise has to be done regarding the antenna performance. According to equation 4.1, the substrate thickness for RT/Duroid 5880 should be equal to or greater than 4.3mm to achieve better bandwidth. Unfortunately, the maximum available thickness for this substrate is 3.175mm. The lower thickness will cause a slight decrease in antenna bandwidth.

5.4.1 Simulated Results

5.4.1.1 Single Element

The new U-slot microstrip patch antenna is designed using empirical formulas presented in section 4.5.1 with new substrate thickness and dielectric values. Necessary tuning is also performed to optimize the design according to the desired performance. The dimensions of the optimized antenna are shown in Table 5.3 and it ADS Momentum layout is shown in Fig. 5.12. It can be noticed that the new antenna design has larger dimensions than the antenna designed for TMM3 substrate. This is because the patch antenna dimensions are inversely proportional to the substrate dielectric constant, as mentioned in Balanis [13].

Table 4: Dimensions of optimized single element dual-band U-slot patch antenna for RT/Duroid 5880

U-Slot Microstrip Patch Antenna							
W	L	C	D	E	F	H	y_P
72	47	21.5	37	2.5	2.5	6	5

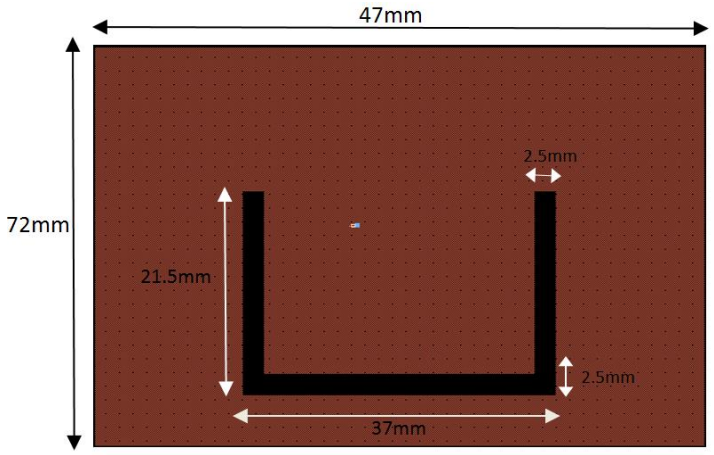

Figure 5.12: Layout of optimized dual-band U-Slot patch antenna for RT/Duroid 5880

The reflection coefficient (S_{11}) or return loss plot of the above antenna is shown in Fig. 5.13. S_{11} at 2.1GHz and 3.5GHz is 25.915dB and 28.610dB respectively. These values of S_{11} at both the frequencies suggest that the antenna has good impedance matching. The 10dB bandwidth for 2.1GHz band comes out to be 52MHz and for 3.5GHz band it is 65MHz. The obtained bandwidths are sufficient for the antenna to be used for LTE because for a 2 x 2 MIMO LTE transmission is done on 20MHz bandwidth (as mentioned in chapter 1). The impedance loop

plot of the optimized antenna is shown in Fig. 5.14. The impedance at the feed point for 2.1GHz and 3.5GHz frequency bands is shown by markers *m1* and *m2*, respectively. The impedance values show good matching between feed point and coaxial probe.

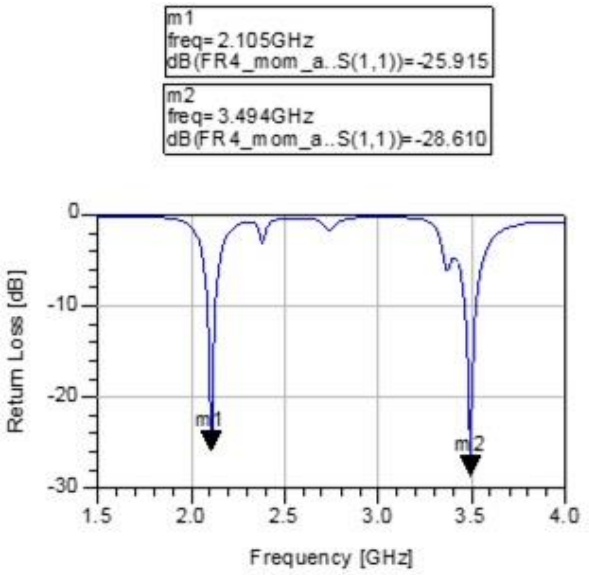

Figure 5.13: Optimized dual-band U-slot patch antenna for RT/Duroid 5880 reflection coefficient – S_{11}

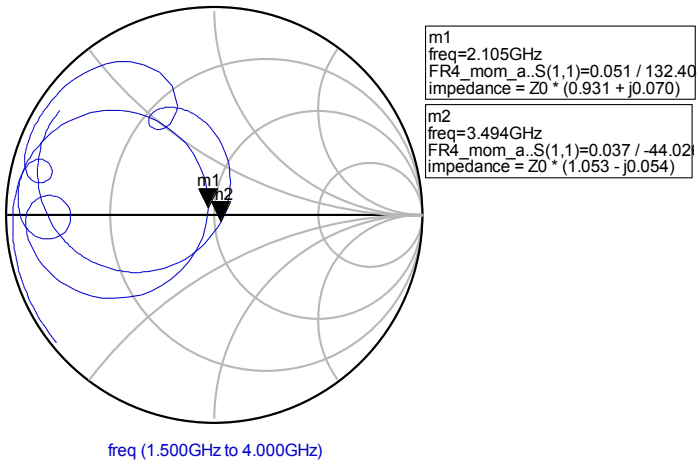

Figure 5.14: Impedance loop plot of optimized patch for RT/Duroid 5880 on Smith chart

Fig. 5.15 shows the antenna gain and directivity. As indicated by marker *m1*, the gain at 2.1GHz is above 7.34dBi. For 3.5GHz, the gain is found to be 5.6dBi. As shown in Fig. 5.16, the antenna has an efficiency of 93% at 2.1GHz which is considered to be a good antenna, radiating most of the incoming radio-frequency power. For 3.5GHz, it is found to be 78%.

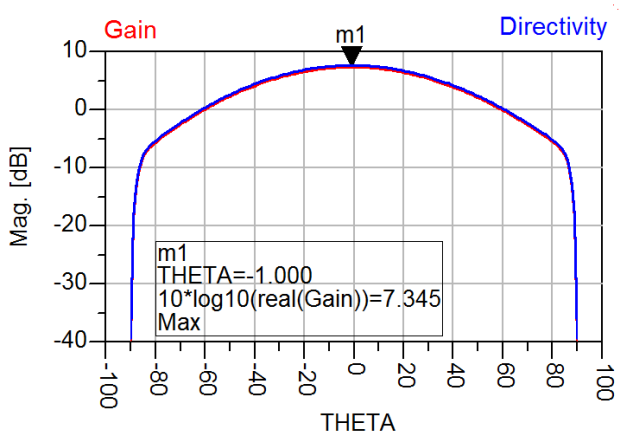

Figure 5.15: U-slot rectangular patch antenna for RT/Duroid 5880 single element antenna gain at 2.1GHz

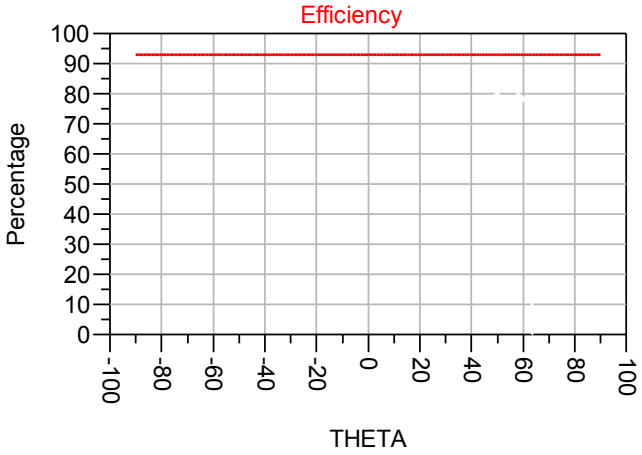

Figure 5.16: U-slot rectangular patch antenna for RT/Duroid 5880 single element efficiency at 2.1GHz

5.4.1.2 2x2 U-Slot Patch Array

Fig. 5.17 shows the configuration of the antenna array. The dimensions of each of the four antenna elements are similar to that in Fig. 5.12. Each element is fed by a separate port and edge-to-edge separation between elements is 10mm. The theoretical and analytical studies about the effect of inter-element distance on the capacity of MIMO systems are presented in [38]. Studies performed in [39] show that for MIMO antennas, maximum efficiency can be obtained at an inter-element distance of 0.4λ or above. However, good results have been reported at a separation of 10mm [40, 41].

The reflection coefficient plots for each of the element in the the 2 x 2 array antenna are shown in Fig. 5.18. The values of the reflection coefficient of four elements S_{11}-S_{44} at 2.1GHz frequency are 60dB, 50dB, 38dB and 41dB, respectively, and that for the 3.5GHz frequency are 32dB, 26dB, 28dB and 34dB, respectively. These values reflect very good impedance matching

for the 2x2 array antenna configuration. The antenna has an efficiency of 97%, as shown in Fig. 5.18, which suggests an excellent radiated to input radio-frequency power ration.

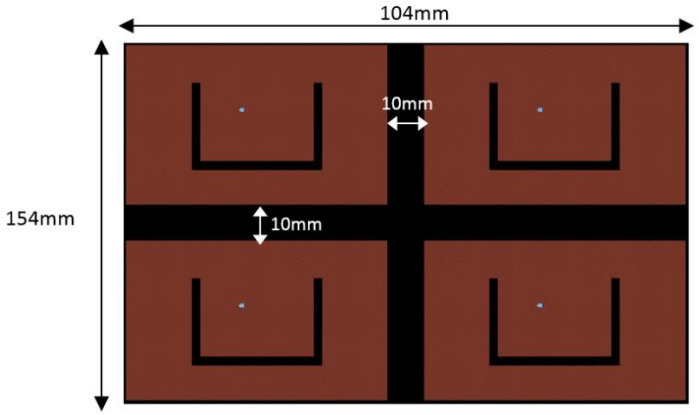

Figure 5.17: Dual-band 2 × 2 U-slot rectangular patch antenna array for RT/Duroid 5880

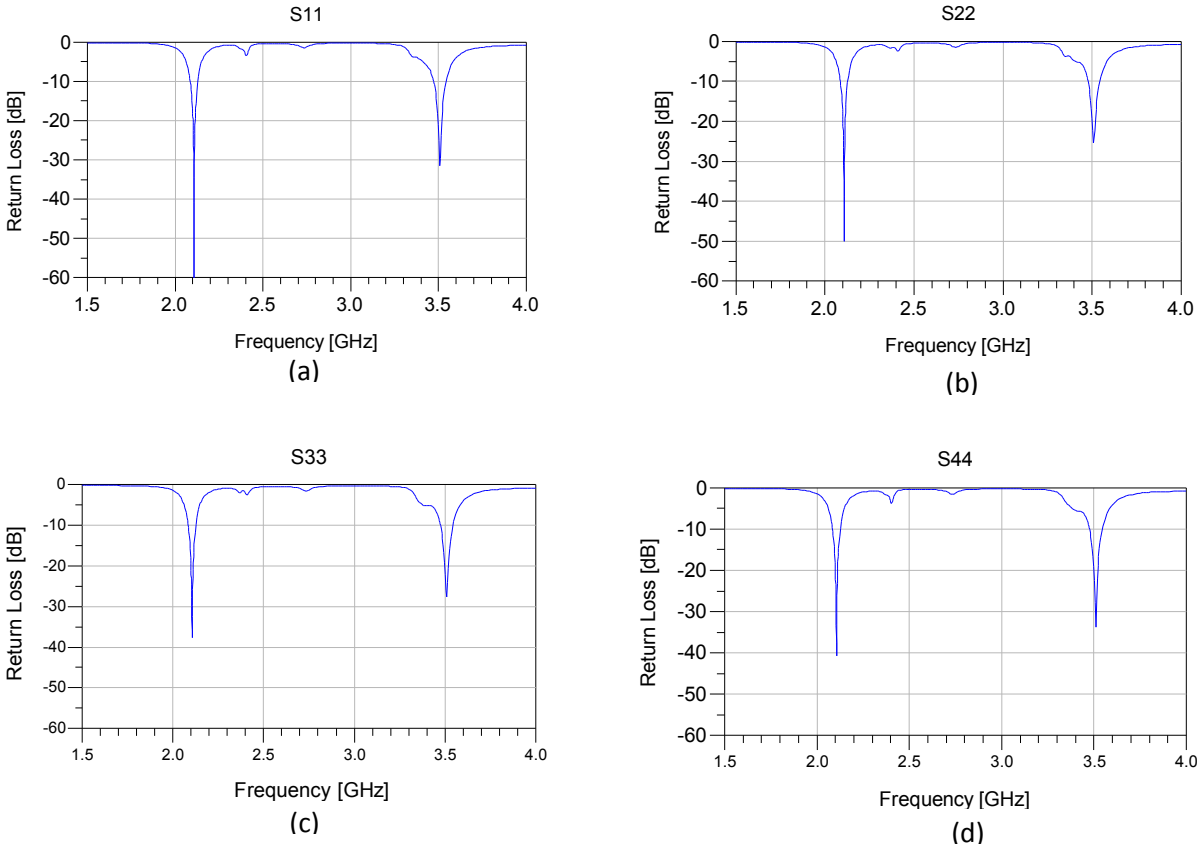

Figure 5.18: 2 × 2 U-slot rectangular patch antenna array for for RT/Duroid 5880 reflection coefficients – S_{11}-S_{44} (a) Reflection coefficient of element-1 – S_{11} (b) Reflection coefficient of element-2 – S_{22} (c) Reflection coefficient of element-3 – S_{33} (d) Reflection coefficient of element-4 – S_{44}

The gain and directivity plots of the 2 x 2 antenna array are shown in Fig. 5.19. The resultant gain of the four antenna elements at 2.1GHz is found to be 11dBi, with two side lobes. These side lobes are very much small as compared with the main lobe of the antenna. The gain at 3.5GHz is found to be 7.6dBi.

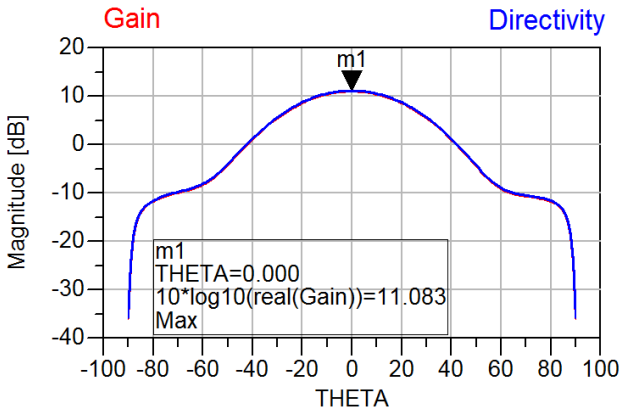

Figure 5.19: 2x2 U-slot rectangular patch antenna for RT/Duroid 5880 directivity and gain at 2.1GHz

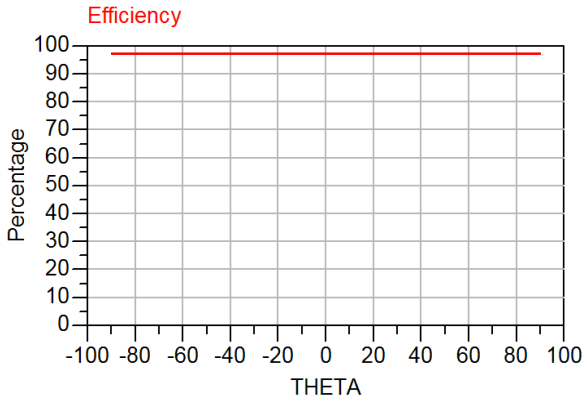

Figure 5.20: 2x2 U-slot rectangular patch antenna array for RT/Duroid 5880 efficiency at 2.1GHz

5.4.2 Measured Results

The simulation results of the 2 x2 U-slot microstrip patch antenna array show that the designed antenna is suitable for use with a MIMO based communication system. However, the software simulations are not a formal justification for a proposed antenna solution. For an antenna to be justified for a practical use, it must be fabricated and tested in real-time environment. For this purpose, the antennas are fabricated and tested to prove our concept and provide a justification for the claim of achieving a dual-band antenna array using U-slotted microstrip

patch configuration for LTE and MIMO applications. The picture of fabricated antenna array is shown in Fig. 2.21.

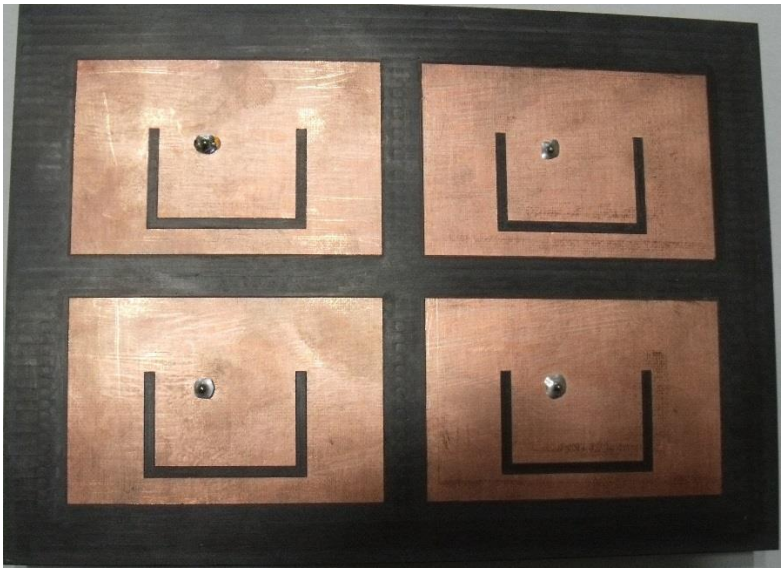

(a)

(b)

Figure 2.21: Fabricated 2 x 2 U-slot rectangular patch antenna array for RT/Duroid 5880
(a) Front view (b) Back view

After fabrication, the antenna reflection coefficient was measured on vector network analyzer (VNA). The VNA is a two-port network and can measure the S-parameters one-by-one for every single antenna element. The measured reflection coefficient plots of the fabricated 2 x2 antenna array are shown in Fig. 5.22. The values of the reflection coefficient of four all the

four elements S_{11}-S_{44} at 2.1GHz frequency are 27.00dB, 27dB, 18.53dB and 26.73dB, respectively, and that for the 3.5GHz frequency are 23.72dB, 23.72dB ,27.95 and 25.10dB, respectively. These values shows that the fabricated antenna array feed points have a very good impedance matching.

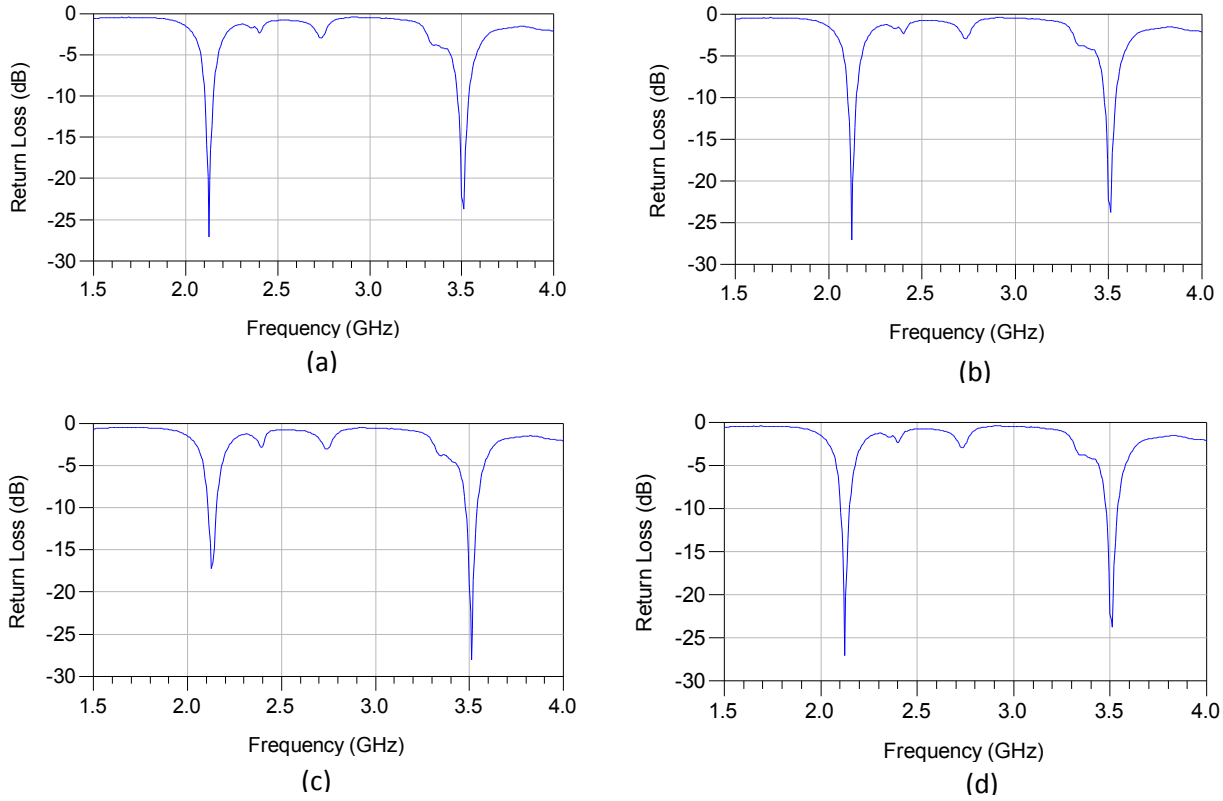

Figure 5.22: 2 × 2 U-slot rectangular patch antenna array for for RT/Duroid 5880 measured reflection coefficients – S_{11}-S_{44} (a) Reflection coefficient of element-1 – S_{11} (b) Reflection coefficient of element-2 – S_{22} (c) Reflection coefficient of element-3 – S_{33} (d) Reflection coefficient of element-4 – S_{44}

The radiation pattern measurements of the fabricated antenna array were performed in anechoic chamber. The radiation patter of all the antenna elements was measured and only one of them is shown here because all the elements are identical. Fig. 5.23 shows the 3D radiation pattern of the antenna at 2.1GHz frequency band. The main lobe is directed upwards with the ground plane at the base of the figure. It can be seen that the main lobe is directional. The intensity of the radio-frequency power on the pattern is shown by different colors. The red portion shows high intensity of power while yellow and green show comparatively low intensity. The radiation pattern had no back lobe. The 2D radiation pattern is shown in Fig. 5.24.

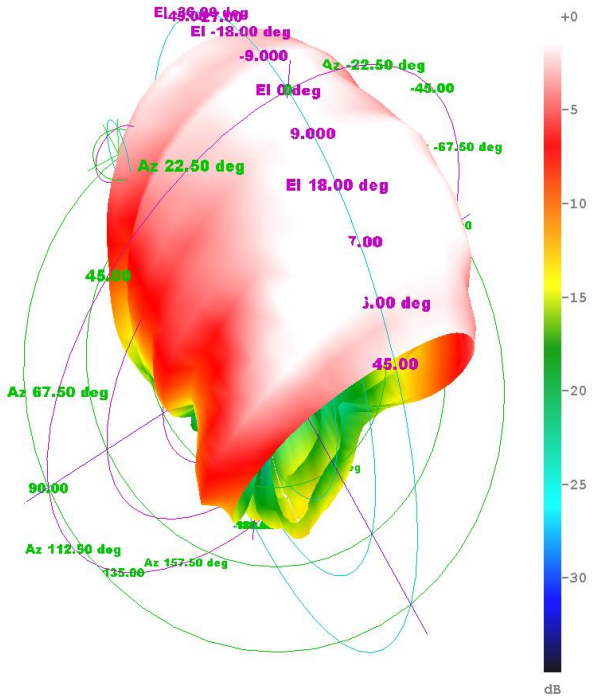

Figure 5.23: Measured 3D radiation pattern of fabricated antenna

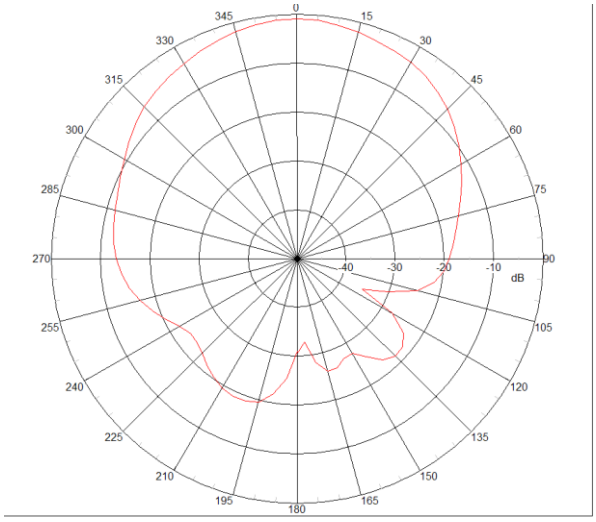

Figure 5.24: Measured 2D radiation pattern of fabricated antenna

5.5 Comparison Between simulated and Measured Results

It is necessary to compare the simulated and measured antenna results in order to check quality of fabrication and difference between modeled antenna and its real-time

implementation. For this purpose, the simulation and measurement results for each of the antenna elements is combined and plotted in a single graph. The scale for all the four graphs is kept constant. Fig 5.25 shows the comparison plots of reflections coefficients of all four antenna elements for both the desired frequency bands. The summarized values of this graph are given in Table 5. The comparison between the two center frequencies (2.1GHz and 3.5GHz) of each of the antenna elements is given in Table 6.

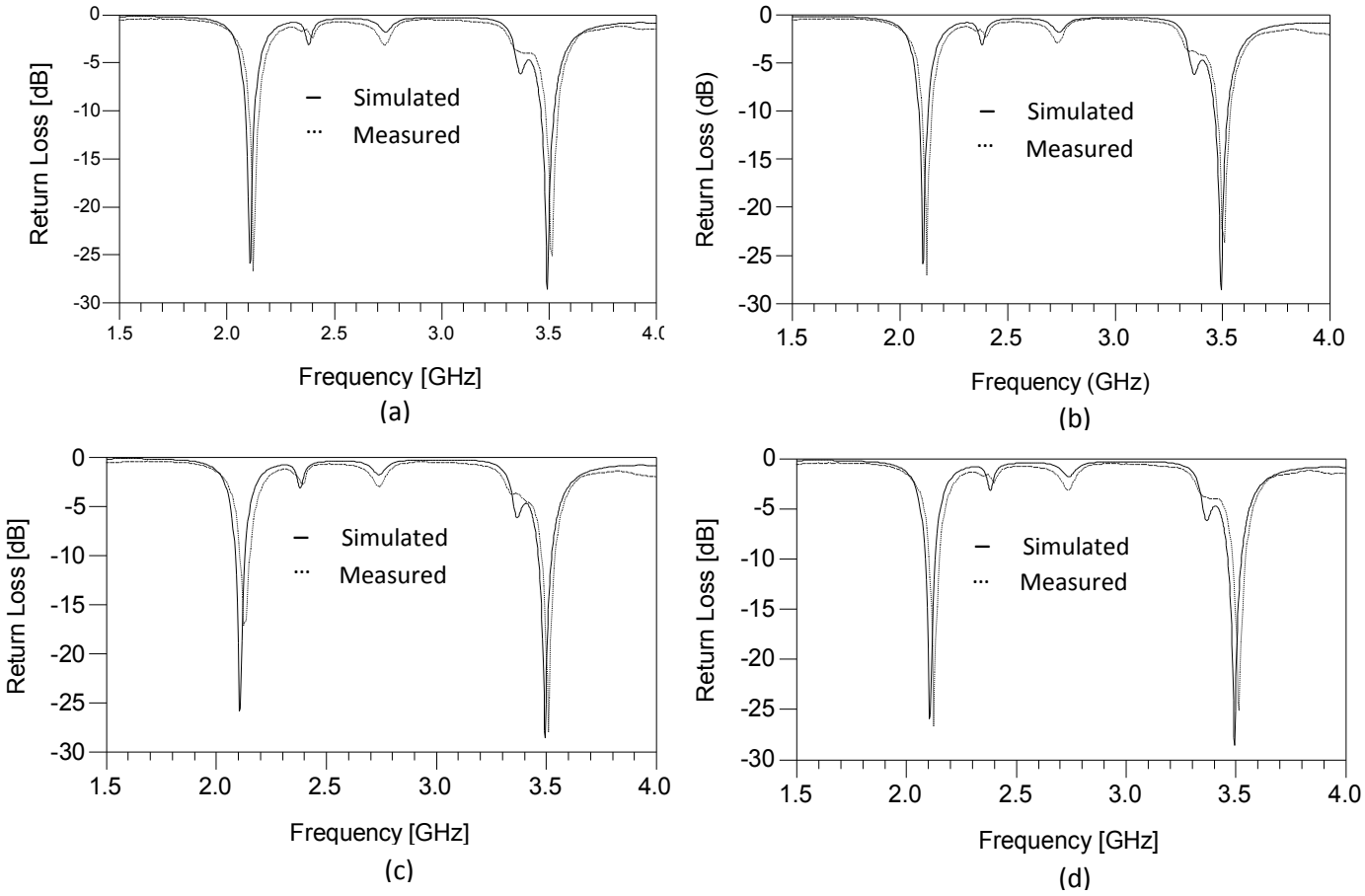

Figure 5.25: Comparison of 2 × 2 U-slot rectangular patch antenna array elements simulated and measured reflection coefficients – S_{11}-S_{44} (a) Reflection coefficient of element-1 – S_{11} (b) Reflection coefficient of element-2 – S_{22} (c) Reflection coefficient of element-3 – S_{33} (d) Reflection coefficient of element-4 – S_{44}

From these comparison plots, it can be seen that the measured return loss is almost identical to the simulated plot, with only a slight difference. This shows the accuracy of the fabrication and coaxial feed.

Table 5: Comparison of simulated and measured reflection coefficients of 2 × 2 U-slot rectangular patch antenna array – S_{11}-S_{44}

2 x 2 U-slot Microstrip Patch Antenna Array								
	Element-1 (S11) [dB]		**Element-2 (S22) [dB]**		**Element-3 (S33) [dB]**		**Element-4 (S44) [dB]**	
	Simulated	Measured	Simulated	Measured	Simulated	Measured	Simulated	Measured
2.1GHz Band	60	27	50	27	38	18.53	41	26.73
3.5GHz Band	32	23.72	26	23.72	38	27.95	34	52.1

Table 6: Comparison of center frequencies for modelled and fabricated 2 x 2 U-slot rectangular patch antenna array elements

2 x 2 U-slot Microstrip Patch Antenna Array								
	Element-1 Center Frequency (GHz)		**Element-2 Center Frequency (GHz)**		**Element-3 Center Frequency (GHz)**		**Element-4 Center Frequency (GHz)**	
	Modelled	Measured	Modelled	Measured	Modelled	Measured	Modelled	Measured
2.1GHz Band	2.1	2.12	2.1	2.12	2.1	2.12	2.1	2.12
3.5GHz Band	3.5	3.51	3.5	3.51	3.5	3.51	3.5	3.51

Chapter 6

Conclusion, Comparison and Future Work

6.1 Conclusion

4G Long Term Evolution (LTE) is the most advanced and fastest mobile communication standard. It requires efficient multiple input multiple output (MIMO) antennas to work. LTE is not yet deployed in Pakistan. This thesis focused on developing an effective dual-band MIMO antenna system designed for LTE Pakistan frequencies to promote its deployment. The planar antennas are very popular due to their small size, light weight, low profile nature and most importantly the low cost. The U-slot microstrip patch antenna was selected to achieve our target of designing a low-cost dual-band MIMO antenna that can provide application diversity. The antenna works on two LTE bands; 2.1GHz and 3.5GHz. U-slot design equations were used to get approximate parameters and some tuning methods were used to achieve accurate results. Agilent ADS was used to simulate and optimize the designed antennas. The original antennas were designed using Rogers TMM3 substrate but due to some procurement problems, it was replaced by RT/Duroid 5880 substrate which is comparatively cheaper. The 2 x 2 antenna array was get fabricated and tested. The measured results are very good with only minor difference. The bandwidth is sufficient to use the antenna for a practical application. Overall, there is a good agreement between the simulated and measured results. This research work justified the proposed concept of a multi-application MIMO antenna.

6.2 Comparison

The results of the proposed antenna array are compared with the researches in the same area done in recent years. The comparison of the designed antenna with different dual-band U-slot antenna performance parameters is given in Table 7. It can be noticed that the proposed antenna is in good match with the works with a significant improvement in antenna gain.

Table 7: Comparison of proposed research work with recently published U-slot dual-band antennas

Antenna Type	Feeding	Frequency	S_{11} (dB)	Bandwidth	Gain (dBi)	Reference
U-slot microstrip patch	Line feed	3.5GHz & 5.5GHz	-22 & -28	2.9% & 7.5%	1.5	[43]
Line-slot patch	Line feed	2.6GHz & 3.5GHz	-18 & -24	5.7% &10.6%	4.1	[44]
U-slot patch (1x4 array)	Probe feed	3.5GHz & 5GHz	-24 & -21	2% & 1.8%	9.5	[45]
Proposed antenna (2x2 array	Probe feed	2.1GHz & 3.5GHz	-28 &-30	2.6% & 2%	11.1 (Efficiency: 97%)	This work

6.2 Future Recommendations

This research work can serve as a guideline for the future research students who are interested in and have an innovative approach towards the field of smart antenna designing for real-life applications. Following research recommendations have been presented for further improvements in the proposed antenna.

- Adding another U-slot will make antenna radiate at three frequencies. This will provide more application diversity.
- A substrate with high dielectric value can be used to reduce the patch size which will make antenna smaller in size and suitable for miniature mobile devices.
- Antenna array can be designed for other mobile communication standards such as 4G WiMAX and MIMO WiFi.
- Different types of feeding networks can be used by designing linear arrays to increase the impedance bandwidth such as quarter wave transmission line feeding.
- The beam of the antenna array can be steered using phase shifters to make the smart antenna. Beam-steering helps transmitting the power in right direction, improving SNR and reduce the peer link interference.

- Besides, other types of slots can be introduced in the rectangular patch antenna such as C, E, F, etc. Each type of slot provides different antenna behavior and multiple resonances.
- Another way of improving the bandwidth is that the mutual interference of the patch elements is reduced by ensuring suitable separation among them.

Appendix A

This table is taken from [42] for reference in this thesis.

LTE Frequency Bands									
Band	Name	**Bandwidth (MHz)**	Downlink (MHz)		Uplink (MHz)		Duplex spacing (MHz)	Equivalent UMTS band	Geographical Area
			Low Earfcn	High Earfcn	Low Earfcn	High Earfcn			
FDD									
1	IMT 2100	**60**	2110 0	2170 599	1920 18000	1980 18599	190	1	EMEA
2	PCS 1900	**60**	1930 600	1990 1199	1850 18600	1910 19199	80	2	NAR
3	DCS 1800	**75**	1805 1200	1880 1949	1710 19200	1785 19949	95	3	
4	AWS	**45**	2110 1950	2155 2399	1710 19950	1755 20399	400	4	NAR
5	US 850 Cellular	**25**	869 2400	894 2649	824 20400	849 20649	45	5	NAR
6	UTRA only	**10**	875 2650	885 2749	830 20650	840 20749	45	6	
7	2.6 GHz	**70**	2620 2750	2690 3449	2500 20750	2570 21449	120	7	EMEA
8	GSM 900	**35**	925 3450	960 3799	880 21450	915 21799	45	8	
9	1700 MHz	**35**	1844.9 3800	1879.9 4149	1749.9 21800	1784.9 22149	95	9	Japan
10	AWS Extended	**60**	2110 4150	2170 4749	1710 22150	1770 22749	400	10	
11	Japan 1500 Lower	**20**	1475.9 4750	1495.9 4949	1427.9 22750	1447.9 22949	48	11	Japan
12	US 700 Lower, A-C	**17**	729 5010	746 5179	699 23010	716 23179	30	12	NAR
13	US 700 Upper, C	**10**	746 5180	756 5279	777 23180	787 23279	-31	13	NAR
14	US Public Safety	**10**	758 5280	768 5379	788 23280	798 23379	-30	14	NAR
17	US 700 Lower, B-C	**12**	734 5730	746 5849	704 23730	716 23849	30		NAR
18	Japan 800 Lower	**15**	860 5850	875 5999	815 23850	830 23999	45		Japan
19	Japan 800 Upper	**15**	875 6000	890 6149	830 24000	845 24149	45	19	Japan
20	Europe 800 EDD	**30**	791 6150	821 6449	832 24150	862 24449	-41	20	EMEA

LTE Frequency Bands									
Band	Name	**Bandwidth (MHz)**	Downlink (MHz)		Uplink (MHz)		Duplex spacing (MHz)	Equivalent UMTS band	Geographical Area
			Low Earfcn	High Earfcn	Low Earfcn	High Earfcn			
21	Japan 1500 Upper	**15**	1495.9 6450	1510.9 6599	1447.9 24450	1462.9 24599	48	21	Japan
22	3.5 Ghz	**80**	3510 6600	3590 7399	3410 24600	3490 25399	100	22	
23	S-Band 2 GHz	**20**	2180 7500	2200 7699	2000 25500	2020 25699	180		NAR
24	L Band	**34**	1525 7700	1559 8039	1626.5 25700	1660.5 26039	-101.5		NAR
25	PCS 1900 + G block	**65**	1930 8040	1995 8689	1850 26040	1915 26689	80	25	NAR
26	US 850 Extended	**35**	859 8690	894 9039	814 26690	849 27039	45	26	NAR
27	US 800 SMR	**17**	852 9040	869 9209	807 27040	824 27209	45		NAR
28	700 MHz APAC	**45**	758 9210	803 9659	703 27210	748 27659	55		APAC
29	US 700 Lower, D-E	**11**	717 9660	728 9769	n/a	n/a	DL only		NAR
TDD									
33	TDD 2000	**20**	1900 36000	1920 36199			TDD		
34	TDD 2000 Europe	**15**	2010 36200	2025 36349			TDD		EMEA
35	TDD PCS Uplink	**60**	1850 36350	1910 36949			TDD		NAR
36	TDD PCS Downlink	**60**	1930 36950	1990 37549			TDD		NAR
37	TDD PCS Center gap	**20**	1910 37550	1930 37749			TDD		NAR
38	TDD 2.6 GHz	**50**	2570 37750	2620 38249			TDD		China
39	China TDD 1.9 GHz	**40**	1880 38250	1920 38649			TDD		China
40	China TDD 2.3 GHz	**100**	2300 38650	2400 39649			TDD		China
41	TDD 2.5 GHz	**194**	2496 39650	2690 41589			TDD		NAR
42	TDD 3.4 GHz	**200**	3400 41590	3600 43589			TDD		
43	TDD 3.6 GHz	**200**	3600 43590	3800 45589			TDD		
44	TDD 700 APAC	**100**	703 45590	803 46589			TDD		APAC

References

[1] G. J. Foschini, “Layered space-time architecture for wireless communication in a fading environment when using multi-element antennas,” *Bell Labs Technical Journal*, pp 41-59, autumn 1996.

[2] L. Liu, R. Chen, S. Geirhofer, K. Sayana, Z. Shi and Y. Zhou, “Downlink MIMO in LTE-Advanced: SU-MIMO vs. MU-MIMO,” IEEE Comm. Mag., vol. 50, no.2, pp.140-147, February 2012.

[3] A. Paulraj, D. Gore, R. Nabar, and H. Bolcskei, “An overview of MIMO communications - a key to gigabit wireless,” Proceedings of the IEEE, vol. 92, no. 2, pp. 198 – 218, Feb. 2004.

[4] Martin Sauter, *Beyond 3G – Bringing Networks, Terminals and the Web Together*, John Wiley & Sons Ltd, 2009.

[5] Advanced Design System, 2008 Momentum Software Manual, Agilent Technologies, CA: Palo Alto, 2008.

[6] Q. Li, G. Li, W. Lee, M. il Lee, D. Mazzarese, B. Clerckx, and Z. Li, “MIMO techniques in WiMAX and LTE: a feature overview,” IEEE Commun. Mag., vol. 48, no. 5, pp. 86 –92, May 2010.

[7] S. Sesia, I. Toufik and M. Baker, *LTE - The UMTS Long Term Evolution: From Theory to Practice*, John Wiley & Sons, Ltd, Chichester, UK, 2009.

[8] J. Lee, J.-K. Han et al., “MIMO Technologies in 3GPP LTE and LTE-Advanced,” EURASIP Journal on Wireless Communications and Networking, vol. 2009, March 2009.

[9] http://www.3gpp.org/LTE

[10] Altman, Zwi; Wiart, Joe; Mittra, Raj. 1998. Design of high gain dipole antennas using the genetic algorithm. IEEE Antennas and Propagation Society International Symposium. 1998. Volume 1. Pages 30--33.

[11] Msc. Thesis, “Design and Simulation of Microstrip Phase Array Antenna using ADS,” Linnaeus University, 2011.

[12] Stutzman, W.L. and Thiele, G.A., Antenna Theory and Design, John Wiley & Sons, Inc, 1998.

[13] Balanis, C.A., Antenna Theory: Analysis and Design, John Wiley & Sons, Inc, 1997.

[14] N. J. Kolias, R. C. Compton, J. P. Fitch and D. M. Pozar, Antenna, CRC Press, 2000.

[15] Makarov, S.N., Antenna and EM Modeling with MATLAB, John Wiley & Sons, Inc, 2002.

[16] Saunders, S.R., Antennas and Propagation for Wireless Communication Systems, John Wiley & Sons, Ltd, 1999.

[17] Kumar, G. and Ray, K.P., Broadband Microstrip Antennas, Artech House, Inc, 2003.

[18] Garg, R., Bhartia, P., Bahl, I., Ittipiboon, A., Microstrip Antenna Design Handbook, Artech House, Inc, 2001.

[19] Balanis, C.A., Advanced Engineering Electromagnetics, John Wiley & Sons, New York, 1989.

[20] Hammerstad, E.O., "*Equations for Microstrip Circuit Design*," Proc. Fifth European Microwave Conf., pp. 268-272, September 1975.

[21] James, J.R. and Hall, P.S., Handbook of Microstrip Antennas, Vols 1 and 2, Peter Peregrinus, London, UK, 1989.

[22] Bahl, I.J. and Bhartia, P., Microstrip Antennas, Artech House, Dedham, MA, 1980.

[23] T. Huynh, K. F. Lee, "*Single-layer single-patch wideband microstrip antenna*," *Electronics Letters*, vol. 31, pp. 1310-1312, Aug. 1995.

[24] David C. Jenn, lecture notes for Antennas and Propagation, unpublished.

[25] Y. X. Guo, K. M. Luk, K. F. Lee and Y. L. Chow, "*Double U-slot rectangular patch antenna*," *Electronics Letters*, vol. 34, pp. 1805-1806, Sept. 1998.

[26] T. Huynh, K. F. Lee, "*Single-layer single-patch wideband microstrip antenna*," *Electronics Letters*, vol. 31, pp. 1310-1312, Aug. 1995.

[27] K. F. Tong, K. M. Luk, K. F. Lee and R. Q. Lee, "*A broad-band U-slot rectangular patch antenna on a microwave substrate*," *IEEE Trans. Antennas Propag*., vol. 48, pp. 954-960, Jun. 2000.

[28] K. F. Lee, K. N. Luk, K. M. Mak and S. L. D. Yang, "*On the use of U-slots in the design of dual-and triple-band patch antennas*," *IEEE Antennas Wireless Propag. Lett*., vol. 7, pp. 645-747, Dec. 2008.

[29] K. F. Lee, K. M. Suk, T. Mang and S. Yand, "*Dual and triple band stacked patch antennas with U-slots*," Proceedings of Fourth Europen Conference on Antennas and Propagation (EuCAP), Barcelona, Spain, 2010, pp. 1-5.

[30] M.S.c. Thesis, "*Design of a compact microstrip patch antenna for use in weireless/cellular devices*," pp. 44, The Florida State University, 2004.

[31] S. Weigand, G. H. Huff, K. H. Pan, J. T. Bernhard, "*Analysis and design of broad-band single layer rectangular U-slot mirostrip patch antennas*," *IEEE Transactions on Antennas and Propagation*, vol. 51, no. 3, March 2003.

[32] V. Natarajan, D. Chatterjee, "*An Empirical Approach for Design of Wideband, Probe-fed, U-slot Microstrip Patch Antennas on Single-layer, Infinite, Grounded Substrates*," ACES Journal, vol. 18, no. 3, November 2003.

[33] V. Natarajan, D. Chatterjee, "*An empirical approach for design of wideband, probe-fed, U-slot microstrip patch antennas on single layer, infinite ground substrates*," *ACES Journal*, vol. 18, no. 3, Nov. 2003.

[34] V. Natarajan, E. Chettiar, D. Chatterjee, "*Performance of two empirical techniques for optimized design of wideband, U-slot antennas using commercial CAD tools*," IEEE antennas and propagation and URSI/USNC symposium digest, vol. 3, Monterey, California, June 2004.

[35] Y. L. Chow and C. W. Fung, "*The City University logo patch antenna*," in Asia-Pacific Microwave Conf. Proc., vol. 1, 1997, pp. 229–232.

[36] http://www.rogerscorp.com/documents/728/acm/TMM-Thermoset-laminate-data-sheet-TMM3-TMM4-TMM6-TMM10-TMM10i.aspx

[37] Holloway, DeLyser, German, McKenna & Kanda, "*Comparison of Electromagnetic Absorber Used In Anechoic and Semi-Anechoic Chambers For Emissions and Immunity Testing of Digital Devices*," IEEE Transactions on Electromagnetic Compatibility, February, 1997.

[38] Abouda, A. A. and S. G. H¨ aggman, "*Effect of mutual coupling capacity of MIMO wireless channels in high SNR scenario*," Progress In Electromagnetics Research, PIER 65, 27–40.

[39] S. Pan, S. Durrani and M.E. Bialkowski, "*MIMO capacity for spatial channel model scenarios*," 8th Australian Communications Theory Workshop (AusCTW'07), Adelaide, Australia, Feb 2007.

[40] W. Swelam, M. Ali Soliman, Ali Gomaa, T. E. Taha, "*Compact dual-band microstrip patch array antenna for MIMO 4G communication systems*", in the proceeding of the 2010 IEEE Antennas & Propagation Symp., (IEEE AP-S/URSI 2010), Toronto, Canada, July 11-17, 2010.

[41] K. J. Babu, K. R. Krishna and L. P. Reddy, "*A multi slot patch antenna for 4G MIMO communications*," International Journal of Future Generation Communication and Networking, vol. 4, no. 2, June 2011.

[42] "3GPP TS 36.1.1 E-UTRA: User Eqiupment (UE) radio transmission and reception." 3GPP, A Gobal Initiative. 16 March, 2013. Web. 19 March, 2013.

[43] Kulkarni, N., Mulgi, S. N. and Satnoor, S. K. (2013), Dual notched U—Slots triple band tunable rectangular microstrip antenna. Microw. Opt. Technology Lett., 55: 509–513, March 2013.

[44] Lu, J.-H. and Liu, Y.-H. Novel dual-band design of planar slot array antenna for 4G LTE/WiMAX access points. Microw. Opt. Technol. Lett., 54: 1193–1196, May 2012.

[45] W. Swelam, M. Ali Soliman, Ali Gomaa, T. E. Taha, "*Compact dual-band microstrip patch array antenna for MIMO 4G communication systems*", in the proceeding of the 2010 IEEE Antennas & Propagation Symp., (IEEE AP-S/URSI 2010), Toronto, Canada, July 11-17, 2010.